Novel Properties of a Mouse γ-Aminobutyric Acid Transporter (GAT4)

M.H. Karakossian[1], **S.R. Spencer**[1], **A.Q. Gomez**[1], **O.R. Padilla**[1], **A. Sacher**[2], **D.D.F. Loo**[3], **N. Nelson**[2], **S. Eskandari**[1]

[1]Biological Sciences Department, California State Polytechnic University, Pomona, CA 91768−4032, USA
[2]Department of Biochemistry, The George S. Wise Faculty of Life Sciences, Tel Aviv University, Tel Aviv 69978, Israel
[3]Department of Physiology, David Geffen School of Medicine at UCLA, University of California, Los Angeles, CA 90095−1751, USA

Abstract. We expressed the mouse γ-aminobutyric acid (GABA) transporter GAT4 (homologous to rat/human GAT-3) in *Xenopus laevis* oocytes and examined its functional and pharmacological properties by using electrophysiological and tracer uptake methods. In the coupled mode of transport (Na^+/Cl^-/GABA cotransport), there was tight coupling between charge flux and GABA flux across the plasma membrane (2 charges/GABA). Transport was highly temperature-dependent with a temperature coefficient (Q_{10}) of 4.3. The GAT4 turnover rate (1.5 s^{-1}; −50 mV, 21°C) and temperature dependence suggest physiological turnover rates of 15–20 s^{-1}. No uncoupled current was observed in the presence of Na^+. In the absence of external Na^+, GAT4 exhibited two distinct uncoupled currents. (i) A Cl^- leak current (I_{leak}^{Cl}) was observed when Na^+ was replaced with choline or tetraethylammonium. The reversal potential of (I_{leak}^{Cl}) followed the Cl^- Nernst potential. (ii) A Li^+ leak current (I_{leak}^{Li}) was observed when Na^+ was replaced with Li^+. Both leak currents were inhibited by Na^+, and both were temperature-independent ($Q_{10} \approx 1$). The two leak modes appeared not to coexist, as Li^+ inhibited (I_{leak}^{Cl}). The results suggest the existence of cation- and anion-selective channel-like pathways in GAT4. Flufenamic acid inhibited GAT4 Na^+/Cl^-/GABA cotransport, I_{leak}^{Li}, and I_{leak}^{Cl}, ($K_i \approx 30$ μM), and the voltage-induced presteady-state charge movements ($K_i \approx 440$ μM). Flufenamic acid exhibited little or no selectivity for GAT1, GAT2, or GAT3. Sodium and GABA concentration

Present address for M.H.K.: Department of Neurobiology, David Geffen School of Medicine at UCLA, 10833 Le Conte Avenue, Los Angeles, CA, 90095−1763, USA

Correspondence to: S. Eskandari; email: seskandari@csupomona.edu

jumps revealed that slow Na^+ binding to the transporter is followed by rapid GABA-induced translocation of the ligands across the plasma membrane. Thus, Na^+ binding and associated conformational changes constitute the rate-limiting steps in the transport cycle.

Introduction

Transport of γ-aminobutyric acid (GABA) into neurons and glia is accomplished by plasma membrane Na^+-dependent and Cl^--facilitated GABA transporters. The GABA transporters perform a number of important functions (Borden, 1996; Nelson, 1998; Dalby, 2003; Richerson & Wu, 2003; Conti, Minelli & Melone, 2004). (*i*) They maintain a low resting level of GABA in the brain extracellular fluid and, hence, prevent GABA receptor desensitization. (*ii*) They transport GABA into neurons and glia after its release from nerve terminals and, thus, regulate the concentration and lifetime of GABA in the synapse. (*iii*) They prevent spill-over of the released GABA to surrounding synapses and, therefore, they ensure synaptic specificity. (*iv*) They contribute to synaptic fidelity by transporting GABA back into the axon terminal in order to provide substrate for refilling of synaptic vesicles. Finally (*v*), these transporters may function in reverse to release GABA into the synapse and, thereby, lead to the modulation of synaptic communication. Therefore, as GABA is the most abundant inhibitory neurotransmitter in the brain, the GABA transporters play important roles in a variety of physiological (e.g., inhibitory synapses) as well as pathophysiological (e.g., epilepsy) processes.

Four GABA transporter isoforms have been identified in mammalian tissues (GAT1, GAT2, GAT3, and GAT4), and are widely and differentially distributed in the central nervous system (Borden, 1996; Nelson, 1998; Gadea & López-Colomé, 2001; Chen, Reith & Quick, 2004; Conti et al., 2004). While GAT1 and GAT4 are primarily expressed in the central nervous system, GAT2 and GAT3 are distributed in the brain, as well as in other tissues (e.g., liver and kidney). It has also become evident that the isoforms exhibit substantial functional and pharmacological differences (Borden, 1996; Matskevitch et al., 1999; Krogsgaard-Larsen, Frolund & Frylenvany, 2000; Sacher et al., 2002; Dalby, 2003). Thus, functional differences among the isoforms coupled with differential localization may contribute to unique in vivo roles of the isoforms. In addition, at least in principle, this isoform diversity presents an opportunity for isoform- and region-specific pharmacological modulation of GABAergic neurotransmission.

In order to determine the relative contribution of individual isoforms to GABAergic neurotransmission, as well as to GABA homeostasis in the brain, it is necessary to fully understand the function of all four isoforms. A great deal is known about the functional properties of GAT1 (Mager et al., 1993, 1996; Cammack, Rakhilin & Schwartz, 1994; Hilgemann & Lu, 1999; Lu & Hilgemann, 1999a,b; Deken et al., 2000; Li, Farley & Lester, 2000; Loo et al., 2000; Binda et al., 2002; Fesce et al., 2002; Quick et al., 2004), and our knowledge of GAT2 and GAT3 is slowly growing (Matskevitch et al., 1999; Forlani et al., 2001; Sacher et al., 2002; Grossman & Nelson, 2003; Whitlow et al., 2003). However, the details of the functional characteristics of GAT4 are unknown (Clark et al., 1992; Clark & Amara, 1994; Grossman & Nelson, 2003; Melamed & Kanner, 2004). In addition, to understand the in vivo role of individual isoforms, it is useful to have isoform-specific inhibitors. Unfortunately, specific and high-affinity inhibitors exist only for GAT1 (Borden, 1996; Krogsgaard-Larsen et al., 2000; Dalby, 2003).

Here, we show that GAT4 possesses functional and pharmacological features that diverge from those of other GABA transporter isoforms. In particular, we report that in the absence of external Na^+, GAT4 exhibits Na^+-inhibited anion (Cl^-) and cation (Li^+) leak currents. The properties of the leak currents suggest that they are mediated by channel modes of the transporter. The Cl^- channel mode is not observed in the well-characterized GAT1 isoform. We show that a common chloride channel blocker, flufenamic acid, is a reversible inhibitor of GAT4, and exhibits little or no selectivity for GAT1, GAT2, or GAT3. Finally, by performing concentration jumps, we provide additional evidence that slow Na^+ binding to the transporter is followed by rapid GABA-evoked translocation of the ligands across the plasma membrane.

Materials and Methods

EXPRESSION IN XENOPUS OOCYTES

Stage V-VI *Xenopus laevis* oocytes were injected with 50 ng of cRNA for human GAT1 (hGAT1; SLC6A1), mouse GAT2 (mGAT2), mouse GAT3 (mGAT3), mouse GAT4 (mGAT4), or a mouse GAT3/GAT4 (mGAT3/4) chimeric protein (Nelson, Mandiyan & Nelson, 1990; Liu et al., 1993). The GABA transporter nomenclature adopted here is that of Liu et al. (1993). mGAT2 is homologous to rat/human BGT1 (SLC6A12), mGAT3 is homologous to rat/human GAT-2 (SLC6A13), and mGAT4 is homologous to rat/human GAT-3 (SLC6A11) (Chen et al., 2004). Mouse GAT3/GAT4 chimeric protein (mGAT3/4) was constructed by utilizing a common *Bgl*II restriction site situated after 285 and 300 codons in the reading frames of GAT3 and GAT4, respectively. This position divides the two transporters into two equal parts and allows the construction of a chimeric protein consisting of half of each transporter in tandem (*see* Fig. 6*E*). GAT3/4 was constructed by using the cloned mGAT3 in pGEM-HJ that was cut by *Bgl*II and *Xba*I. A corresponding cDNA fragment was excised from mGAT4 and cloned into the above restriction sites. Like its parental proteins, the mGAT3/4 chimeric protein exhibited Na^+-dependent GABA uptake. After cRNA injection, oocytes were maintained in Barth's medium (in mM: 88 NaCl, 1 KCl, 0.33 $Ca(NO_3)_2$, 0.41 $CaCl_2$, 0.82 $MgSO_4$, 2.4 $NaHCO_3$, 10 HEPES, pH 7.4, and 50 µg/mL gentamicin, 100 µg/mL streptomycin, and 100 units/mL penicillin) at 18°C for up to 21 days until used in experiments. Unless otherwise indicated, experiments were performed at 21 ± 1°C.

EXPERIMENTAL SOLUTIONS

Unless otherwise indicated, experiments were performed in a NaCl buffer containing (in mM): 100 NaCl, 2 KCl, 1 $CaCl_2$, 1 $MgCl_2$, 10 HEPES, pH 7.4. In Na^+-free solutions, NaCl was isosmotically replaced with choline-Cl or tetraethylammonium chloride (TEA-Cl). In experiments in which the Li^+ leak was examined, NaCl was isosmotically replaced with LiCl. In Cl^--free solutions, NaCl, KCl, $CaCl_2$, and $MgCl_2$ were isosmotically replaced with corresponding gluconate salts. GABA and/or pharmacological agents were added to the above solutions as indicated. Stock solutions of GABA transporter and chloride channel blockers were prepared in water, ethanol, or dimethyl sulfoxide (DMSO), and were then diluted in the NaCl buffer as indicated. In control experiments, neither ethanol nor DMSO had an effect on the GABA transporters at concentrations resulting from dilution of the vehicle. All reagents were purchased from Sigma (St. Louis, MO).

GABA UPTAKE IN XENOPUS OOCYTES

Control, hGAT1−, mGAT2−, mGAT3−, mGAT3/4−, or mGAT4-expressing oocytes were incubated for 30 minutes in 200 µM GABA in addition to 22 nM of [³H]-GABA (Amersham BioSciences; Piscataway, NJ). In some experiments, GABA transporter inhibitors or chloride channel blockers were also added to the incubation medium. At the end of the incubation period, oocytes were washed, solubilized in 10% sodium dodecyl sulfate and counted in a liquid scintillation counter (Beckman LS 5000CE; Fullerton, CA).

To determine the relationship between the GABA-evoked current and GABA uptake, uptake experiments were performed

under voltage clamp. The membrane potential was held at -50 mV, and the holding current was continuously monitored. Oocytes were initially incubated in the NaCl buffer until baseline was established. GABA (200 μM) and [³H]-GABA (30 nM) were added to the perfusion solution for 5–10 minutes. At the end of the incubation period, GABA and the isotope were removed from the perfusion solution until the holding current returned to the baseline. The oocytes were removed from the experimental chamber, washed in ice-cold choline-Cl buffer, and solubilized in 10% sodium dodecyl sulfate. Oocyte [³H]-GABA content was determined in a liquid scintillation counter. Net inward charge was obtained from the time integral of the GABA-evoked inward current and correlated with GABA influx in the same cell (Eskandari et al, 1997; Sacher et al, 2002; Whitlow et al, 2003).

ELECTROPHYSIOLOGICAL MEASUREMENTS AND DATA ANALYSIS

The two-microelectrode voltage-clamp technique was used for the recording of whole-cell transporter-mediated currents. Oocytes were voltage-clamped by using the Warner Oocyte Clamp (OC-725C; Warner Instrument, Hamden, CT). In the recording experimental chamber, oocytes were initially stabilized in the NaCl buffer, and the composition of the bath was changed as indicated. In all experiments, the reference electrodes were connected to the experimental oocyte chamber via agar bridges (3% agar in 3 M KCl). For continuous holding-current measurements, currents were low-pass filtered at 1 Hz (LPF 8; Warner Instrument), and sampled at 10 Hz (pCLAMP 8.1, Axon Instruments; Union City, CA).

Substrate-induced steady-state cotransporter currents were obtained from the difference between the steady-state currents in the absence and presence of GABA. The effects of substrate concentration ([GABA]$_0$, [Na$^+$]$_0$, and [Cl$^-$]$_0$) on the steady-state kinetics were determined by non-linear curve fitting of the induced currents (I) to Equation 1:

$$I = \frac{I_{max}^S \cdot [S]^n}{\left(K_{0.5}^S\right)^n + [S]^n} \tag{1}$$

where S is the substrate (GABA, Na$^+$, or Cl$^-$), I_{max}^S is the maximal substrate-induced current, $K_{0.5}^S$ is the substrate concentration at half I_{max}^S (half-maximal concentration), and n is the Hill coefficient. For steady-state current-voltage (I-V) relations, the pulse protocol (pCLAMP 8.1, Axon Instruments) consisted of 400-ms voltage steps from a holding potential of -50 mV to a series of test voltages (V_m) from $+80$ to -148 mV in 19-mV steps. Currents were low-pass filtered at 500 Hz, and sampled at 2 kHz. At each voltage, the steady-state GABA-evoked current was obtained as the difference in steady-state current in the absence and presence of GABA.

To examine the carrier-mediated presteady-state current transients, the pulse protocol consisted of voltage jumps (400 ms) from the holding voltage (-50 mV) to test voltages ranging from $+80$ to -130 mV in 10-mV steps. Unless otherwise indicated, voltage pulses were separated by an interval of at least 4 s in order to allow for complete relaxation of the OFF transients (see Fig. 8) (Sacher et al., 2002; Whitlow et al., 2003). Currents were low-pass filtered at 1 kHz and sampled at 12.5 kHz without averaging. To obtain the transporter presteady-state currents, at each V_m, the total current, $I(t)$, was fitted to Equation 2:

$$I(t) = I_1 e^{-t/\tau_1} + I_2 e^{-t/\tau_2} + I_{SS} \tag{2}$$

where t is time, $I_1 e^{-t/\tau_1}$ is the oocyte capacitive transient current with initial value I_1 and time constant τ_1, $I_1 e^{-t/\tau_2}$ is the transporter transient current with initial value I_2 and time constant τ_2, and I_{SS} is the steady-state current (Loo et al., 1993; Sacher et al., 2002). At

each V_m, the total transporter-mediated charge (Q) was obtained by integration of the transporter transient currents. The charge-voltage (Q–V) relations obtained were then fitted to a single Boltzmann function (Equation 3):

$$\frac{Q - Q_{hyp}}{Q_{max}} = \frac{1}{1 + e^{\left[\frac{-z\delta F(V_m - V_{0.5})}{RT}\right]}} \tag{3}$$

where $Q_{max} = Q_{dep} - Q_{hyp}$ (Q_{dep} and Q_{hyp} are Q at depolarizing and hyperpolarizing limits), z is the apparent valence of the moveable charge, δ is the fraction of the membrane electric field traversed by the charge, $V_{0.5}$ is the V_m for 50% charge movement, F is Faraday's constant, R is the gas constant, and T is the absolute temperature. Subtracted presteady-state current transients (Fig. 7B) were obtained as detailed previously (Sacher et al., 2002). Rapid concentration jumps (Fig. 11) were performed according to a modified version of the method described by Mager et al. (1996).[1] Current records were low-pass filtered at 500 Hz and sampled at 2 kHz.

Data for the inhibition experiments were fitted to Equation 4:

$$\frac{I}{I_0} = \frac{(K_i)^{n'}}{(K_i)^{n'} + [B]^{n'}} \tag{4}$$

where I_0 is the current evoked in the absence of inhibiting agent or blocker (B), I is the current in the presence of a given concentration of blocker, K_i is the inhibitor concentration at which I is 50% of I_0 (apparent half-inhibition constant), and n' is a pseudo Hill coefficient.

Presteady-state and steady-state curve fittings were performed by using either SigmaPlot (SPSS Science; Chicago, IL), or software developed in this laboratory (using a Marquardt-Levenberg algorithm). Where sample sizes are indicated (N), they refer to the number of oocytes in which the experiments were repeated. Reported errors represent the standard error of the mean obtained from data from several oocytes.

TEMPERATURE DEPENDENCE OF GAT4

The temperature dependence of GAT4 GABA-evoked steady-state current was examined at 16–31°C. At temperatures below 16°C, the GABA-evoked current was too small for reliable quantification, and at temperatures above 31°C, the cells became increasingly unstable. For temperatures above the room temperature (>21°C), the bath temperature was adjusted by using a Warner Instrument TC-324B Automatic Temperature Controller and an in-line solution heater (SH-27B; Warner Instrument Hamden, CT). For temperatures below the room temperature (< 21°C), the perfusion solution was pre-chilled to 1°C and then adjusted to the desired temperature using the above-mentioned temperature controller system. The actual temperature in the bath was monitored by a thermistor positioned near the oocyte. The reported temperatures in the oocyte experimental chamber were accurate to ± 0.2°C.

Results

GENERAL STEADY-STATE CHARACTERISTICS OF GAT4

We first present the general steady-state properties of GAT4, as these features have not been documented. GABA transport by GAT4 was strictly Na$^+$-depen-

---

[1]Gomez, A.Q., Lee, W., Chapman, J.V., Errico, M.J., Loo, D.D.F., Eskandari, S. 2005. A novel method for rapid concentration jumps around intact, voltage-clamped *Xenopus laevis* oocytes. Exp. Biol., impress
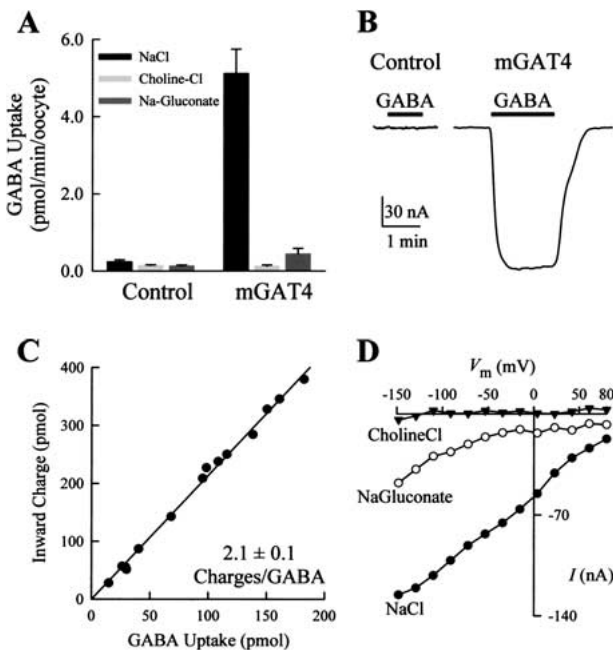
Fig. 1. General steady-state properties of GAT4. (*A*) GABA uptake (200 μM) into GAT4-expressing oocytes was strictly dependent on external Na^+, however, external Cl^- was not absolutely required. The data for each bar represent the mean ± SE from at least 30 control or GAT4-expressing cells. Similar results were obtained with cells from four donor frogs. (*B*) In GAT4-expressing cells, GABA evoked an inward current that was absent in control cells ($V_m = -50$ mV). (*C*) The total charge translocated across the plasma membrane (i.e., time integral of the GABA-evoked inward current) was directly proportional to GABA uptake. The solution contained 200 μM GABA and 30 μM $[^3H]$-GABA. The ratio of net inward charge to GABA uptake obtained in the same cells was 2.1 ± 0.1 charges/GABA ($N = 16$). V_m was −50 mV. (*D*) Similar to GABA uptake, the GABA-induced (200 μM) inward current was strictly dependent on external Na^+, but only partially dependent on external Cl^-. The current-voltage relationship (taken as the difference between values in the presence and absence of GABA) did not saturate at hyperpolarized potentials and approached zero at depolarized potentials.

dent; however, dependence on Cl^- was not absolute (Fig. 1, *A* and *D*). Transport was electrogenic (Fig. 1*B*), and the net charge translocated across the plasma membrane was directly proportional to GABA influx (2.1 ± 0.1 charges/GABA) (Fig. 1*C*). The specific inhibitors of GAT-1, SKF 89976-A and NO-711 (up to 500 μM), had no inhibitory effect on the GAT4 GABA-induced inward current (*not shown*). At −50 mV, the half-maximal concentration for GABA activation of the inward currents was 8.1 ± 1.0 μM ($N = 3$) (Fig. 2*A*). The half-maximal concentration for Na^+ activation of the inward current was 61 ± 2 mM ($N = 3$), and the Na^+ Hill coefficient was 2.4 ± 0.1 ($N = 3$) (Fig. 2*B*). At nominal zero $[Cl^-]_0$, the GABA-evoked current was 24 ± 1% of that at 106 mM Cl^- ($N = 4$) (Fig. 2*C*). The half-maximal concentration for Cl^--enhancement of the inward current was 32 ± 2 mM ($N = 3$).

The Hill coefficient for Cl^--enhancement of the inward currents was 2.0 ± 0.2 ($N = 3$) (Fig. 2*B*). Thus, the steady-state kinetics data suggest that during a typical transport cycle, 1 GABA, ≥2 Na^+, and at least 2 Cl^- ions interact with GAT4.

The GABA-evoked current was highly temperature-dependent (Fig. 3). Figure 3*A* shows GAT4 GABA-evoked (200 μM) responses at 21°C (Fig. 3*A*, *left panel*) and 31°C (Fig. 3*A, right panel*). At 31°C, the maximum GABA-evoked current (I_{max}) was 430 ± 20% of that at 21°C ($N = 8$). Thus, the temperature coefficient (Q_{10}, 21–31°C) was 4.3 ± 0.2 ($N = 8$). Figure 3*B* shows an Arrhenius plot for the temperature dependence of I_{max}. The activation energy (E_a) determined from the slope of the plot was 29 ± 1 kcal/mol ($N = 5$) ($E_a = -slope \times R$, where R is the gas constant, 1.987 cal · mol^{-1} · K^{-1}).

GAT4 HAS AN ANION AND A CATION "LEAK" CONDUCTANCE

As shown above, in the coupled mode of transport (Na^+/Cl^-/GABA cotransport), the GABA-evoked inward current was directly proportional to GABA influx. The fixed ratio of 2 charges/GABA argues against the presence of uncoupled leak pathways during the cotransport cycle. Thus, the data suggest tight coupling between charge flux and GABA flux. In addition, in the presence of Na^+ (absence of GABA), no uncoupled current was observed (*see* Fig. 6*A*). However, in the absence of external Na^+, GAT4 exhibited two distinct uncoupled currents: an uncoupled anion (Cl^-) current and an uncoupled cation (Li^+) current. It will be shown below that these pathways are present only in the absence of external Na^+ and appear not to coexist.

When external Na^+ in bathing medium of GAT4-expressing oocytes was isosmotically replaced with choline or tetraethylammonium (cations that do not interact with GAT4), an inward current was observed (Fig. 4*A*, *middle panel*). A similar observation was obtained when Na^+ was replaced with either choline or TEA, suggesting that it is the absence of Na^+, which gives rise to this current, rather than a specific interaction of choline or TEA with the transporter. This observation is in contrast to that seen in control cells (Fig. 4*A*, *left panel*), cells expressing human GAT1 (hGATl; Fig. 4*A, right panel*) or rat GAT1 (Mager et al, 1996), as well as that seen in oocytes expressing other electrogenic Na^+-coupled transporters (Eskandari et al., 1997; Panayotova-Heiermann et al., 1998; Forster et al., 2002). This current is not altered by GABA (up to 1 mM; *not shown*). Because it is neither evoked nor altered by GABA, the current appears to represent an uncoupled mode of the transporter. As it will be shown that this "leak" current is carried by Cl^-, it is henceforth referred to as I_{leak}^{Cl}. When examined in the
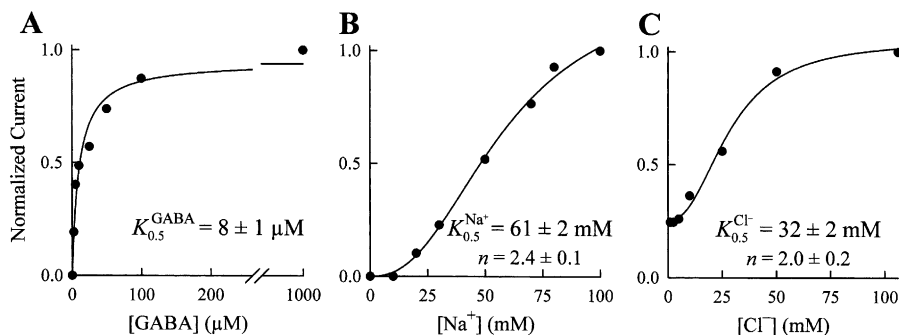
Fig. 2. Steady-state kinetic parameters. (*A*) The GABA-evoked inward current was saturable with a half-maximal concentration ($K_{0.5}^{GABA}$) of 8.1 ± 1.0 μM (100 mM [Na$^+$]$_o$, 106 mM [Cl$^-$]$_o$) (*N* = 3). (*B*) The Na$^+$ dependence of the GABA-evoked (500 μM GABA, 106 mM [Cl$^-$]$_o$) current followed a sigmoidal relationship with a Hill coefficient of 2.4 ± 0.1 (*N* = 4). The half-maximal Na$^+$ concentration ($K_{0.5}^{Na^+}$) was 61 ± 2 mM (*N* = 3). (*C*) In the absence of external Cl$^-$, the current was reduced by ≈75%. Cl$^-$ enhancement of the GABA-evoked (500 μM GABA, 100 mM

[Na$^+$]$_o$) current followed sigmoidal kinetics. The Cl$^-$ concentration required for half-maximal enhancement of the GABA-evoked current was 32 ± 2 mM (*N* = 4). The Hill coefficient for Cl$^-$ enhancement was 2.0 ± 0.2 (*N* = 4). The reported values in panels *A–C* are for V_m = −50 mV. The *lines* in panels *A–C* represent the fit of the data to Equation 1. In panel *C*, an additional linear term was added to account for the non-zero baseline at zero Cl$^-$ concentration.

same cells, the magnitude of I_{leak}^{Cl} was directly proportional to the GABA-evoked steady-state inward current (Fig. 4*B*), suggesting that the appearance of I_{leak}^{Cl}, was in direct correlation with that of the GABA-evoked current and, hence, GAT4 expression at the cell surface. At a holding potential of −60 mV, I_{leak}^{Cl} was 55 ± 4% of the GABA-evoked inward current (Fig. 4*B*) (*N* = 29).

The *I-V* relationship (−150 to + 80 mV) of I_{leak}^{Cl} is shown in Fig. 4*C*. I_{leak}^{Cl} reversed at −29 ± 1 mV (*N* = 3), close to the predicted Cl$^-$ equilibrium potential (−32 mV) under our experimental conditions: [Cl$^-$]$_o$ = 106 mM, and assuming that [Cl$^-$]$_i$ = 30 mM (Cooper & Fong, 2003). In addition, a Nernstian relationship was obtained when the reversal potential (V_{rev}) of I_{leak}^{Cl}, was plotted as a function of the external Cl$^-$ concentration. At all [Cl$^-$]$_o$, V_{rev} closely followed the predicted Nernst equilibrium potential for Cl$^-$. The slope was 56 ± 3 mV per 10-fold change in the external Cl$^-$ concentration (*N* = 4) (Fig. 4*C; lower panel*). Changes in the external K$^+$ or H$^+$ concentration did not lead to alterations of I_{leak}^{Cl} magnitude or reversal potential (*not shown*). Due to the small magnitude of I_{leak}^{Cl}, as well as its sensitivity to external Na$^+$ (*see* Fig. 4*A* and Fig. 4*D*), it was not possible to obtain reliable reversal potentials at different Na$^+$ concentrations.

Sodium led to a concentration-dependent reduction in I_{leak}^{Cl} (Fig. 4*D*). External Na$^+$ reduced I_{leak}^{Cl} with a half-inhibition concentration of 28 ± 2 mM, and a Hill coefficient of 3.0 ± 0.2 (*N* = 4) (Fig. 4*D*). I_{leak}^{Cl} was temperature-independent. At 26°C, the magnitude of the Cl$^-$ leak current was not significantly different from that at 21°C (*N* = 3) (Fig. 4*E*). The Q_{10} (21–26°C) for I_{leak}^{Cl}, was 1.03 ± 0.01 (*N* = 3).

Altogether, the data suggest that GAT4 exhibits a Na$^+$-inhibited Cl$^-$-channel mode. In the absence

of external Na$^+$, the ion permeation pathway forms a Cl$^-$-selective channel. The sensitivity of the channel mode to external Na$^+$ suggests that > 2 Na$^+$ ions interact with GAT4 in a cooperative fashion to occlude the permeation pathway. The small magnitude of I_{leak}^{Cl} suggests that the single-channel conductance and/or the open-state probability are very small.

We note here that the mouse GAT3 isoform exhibits a similar uncoupled current, albeit it is less pronounced (~20% of GABA-evoked current at −60 mV), and is readily detectable only in highly-expressing cells (*not shown*). As shown in Fig. 4*A*, no I_{leak}^{Cl} is observed in GAT1-expressing cells.

The GABA transporters have been shown to exhibit a Na$^+$-inhibited Li$^+$ leak (Mager et al., 1996; Bismuth, Kavanaugh & Kanner, 1997; MacAulay, Zeuthen & Gether, 2002; Grossman & Nelson, 2003; Kanner, 2003). Thus, we examined the Li$^+$ leak current (I_{leak}^{Li}) of GAT4. In these experiments, NaCl in the bath was replaced with an equimolar concentration of LiCl. A typical current-voltage relation is shown in Fig. 5*A*. Consistent with that seen for GAT1 (MacAulay et al., 2002; Kanner, 2003), I_{leak}^{Li} was most pronounced at hyperpolarized membrane potentials, and approached zero at depolarized potentials without reversing. Addition of GABA (up to 1 mM) had no effect on I_{leak}^{Li} (*not shown*). Interestingly, no Cl$^-$ leak current was observed in the presence of 100 mM Li$^+$ (compare *I-V* relationships in Figs. 4*C* and 5*A*). When examined at + 80 mV, I_{leak}^{Li}, was inhibited by Li$^+$ in a concentration-dependent manner with a K_i of 5.5 ± 3.0 mM (*N* = 4) (Fig. 5*B*). Similar to I_{leak}^{Cl}, I_{leak}^{Li} was potently inhibited by Na$^+$ (K_i = 11 ± 2 mM; *N* = 3) (Fig. 5*C*), and was temperature-independent (Q_{10} = 1.01 ± 0.03; *N* = 4) (Fig. 5*D*).

A

B

$$E_a = 29 \pm 1 \text{ kcal/mol}$$

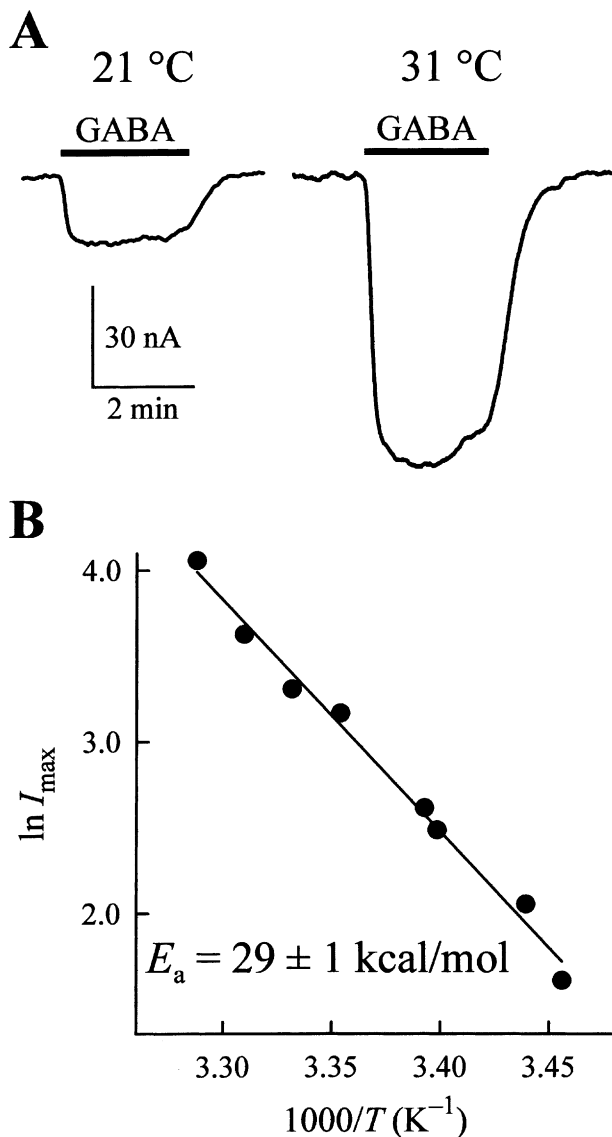**Fig. 3.** GAT4 $Na^+/Cl^-/GABA$ cotransport is highly temperature-dependent. (*A*) GABA-evoked current traces were recorded at 21 (*left panel*) and 31°C (*right panel*) from an oocyte expressing GAT4 ([GABA] = 200 μM; V_m = −50 mV). There was a > 4-fold increase in the GABA-evoked current as the temperature was raised by 10°C. Q_{10} (21–31°C) was 4.3 ± 0.2 (*N* = 8). (*B*) Arrhenius plot for the temperature dependence of GABA-evoked I_{max} (V_m = −50 mV). The temperature of the bath was varied between 16.2 and 31°C. The GABA concentration used (200 μM) was saturating at all temperatures. The line is a linear regression through the data points. The activation energy (E_a) was determined from the slope of the line (E_a = −slope × R, where R is the gas constant). E_a was 29 ± 1 kcal/mol (*N* = 5).

Thus, the data suggest that in the absence of Na^+, the smaller Li^+ ion permeates an apparently cation-selective channel. The data also suggest that Li^+ interaction with the transporter occludes the anion-selective permeation pathway. Both the cation and anion channel-like permeation pathways are occluded upon Na^+ binding to the transporter.

ISOFORM-SPECIFIC PHARMACOLOGICAL BLOCKADE OF GAT4

The chloride leak conductance of GAT4 prompted us to examine the effect of chloride-channel blockers on GAT4 cotransport and leak modes of operation. Interestingly, flufenamic acid, a common chloride-channel blocker, led to complete inhibition of $Na^+/Cl^-/GABA$ cotransport (K_i = 29 ± 7 μM; *N* = 5) (Fig. 6, *A* and *B*), I_{leak}^{Cl}, (K_i = 30 ± 2 μM; *N* = 3) (Fig. 6C), I_{leak}^{Li} (K_i = 23 ± 6 μM; *N* = 3) (Fig. 6D), and the transporter presteady-state charge movements (*see* Fig. 9D). Inhibition was reversible (*not shown*). That the K_i was the same for inhibition of cotransport and channel modes suggests that flufenamic acid probably does not interact with the Na^+ and/or GABA binding sites. When applied alone (in the presence of NaCl), flufenamic acid (500 μM) did not lead to an alteration of the holding current (Fig. 6A; *left trace*), suggesting that no uncoupled current was present in the presence of Na^+.

Flufenamic acid (500 μM) inhibited GABA uptake mediated by GAT4, but had no significant effect on hGAT1, mGAT2, or mGAT3 GABA uptake (Fig. 6E). Interestingly, flufenamic acid did not inhibit an mGAT3/4 chimeric protein. In this chimeric protein, the first 300 residues of mGAT4 have been replaced by the corresponding 285 residues from the closely related mGAT3 isoform (Fig. 6E; *inset*). The data, therefore, suggest that flufenamic acid interaction with GAT4 is in the amino half of the transporter. At 500 μM, flufenamic acid led to a slight inhibition of hGAT1 GABA-evoked inward current (*not shown*), suggesting low-affinity interaction with hGAT1 (K_i >> 500 μM). This effect was not detected at 100 μM. This small interaction was not detected in uptake experiments (Fig. 6E), probably because of the variability seen in the expression level among oocytes.

When tested at 500 μM, other chloride-channel blockers, furosemide, diphenyl-2-carboxylate, and NPPB (5-nitro-2-[3-phenylpropylamino] benzoic acid) had no significant inhibitory effect on GAT4 (*not shown*). Niflumic acid (2-[3-(trifluoromethyl) anilino] nicotinic acid; 500 μM) led to ∼50% inhibition of both GAT1 and GAT4 (*not shown*).

PRESTEADY-STATE CHARGE MOVEMENTS OF GAT4

Similar to that observed for other electrogenic Na^+-coupled transporters, GAT4 exhibited presteady-state current transients (charge movements) induced by voltage pulses (Fig. 7A). Maximum charge movement was observed in the absence of GABA and in the presence of saturating concentrations of Na^+ and Cl^- (*see* Fig. 9). As no charge movements were observed in the absence of external Na^+ (*see* Fig. 9A), the presteady-state transients were isolated from

the capacitive and steady-state components by point-by-point subtraction of the records in the presence and absence of external Na^+ (Fig. 7B) (Mager et al., 1993; Hazama, Loo & Wright, 1997; Sacher et al., 2002). The subtracted records revealed a rapid rising phase of the charge movements followed by slower mono-exponential decay to the steady state (Fig. 7B) (Lu & Hilgemann, 1999b; Sacher et al., 2002). The slow component (Q_{slow}) accounts for >98% of the charge moved and will be the focus of the following discussion. At each test voltage, the integral of the carrier-mediated current transients for the ON response (in Fig. 7B) yielded the charge-voltage (Q_{ON}-V) relation (Fig. 7C). The voltage for 50% charge translocation ($V_{0.5}$) was 18 ± 1 mV ($N = 26$), and the effective valence of the moveable charge ($z\delta$) was 1.8 ± 0.1 ($N = 26$). The maximum charge moved (Q_{max}) is a measure of the total number of functional transporters in the plasma membrane (Eskandari et al., 2000) and, thus, depended on the level of GAT4 expression at the cell surface (see Fig. 10). The relaxation of the ON transients followed a single exponential function. The decay time constant plotted as a function of the test voltage (τ_{ON}-V relation) followed a bell-shaped function with a maximum value of 114 ± 7 ms ($N = 26$) (Fig. 7D). The voltage at maximum τ_{ON} (21 ± 3 mV; $N = 26$) was similar to the $V_{0.5}$ of the Q-V curve (18 ± 1; Fig. 7C). These results suggest that the voltage-induced transitions may be adequately approximated as a two-state process governed by one dominant voltage-dependent rate-limiting step (Loo et al., 1993). The data further suggest the movement of a minimum of two elementary charges within the membrane electric field.

The relaxation of the OFF transients was considerably slower than that of the ON transients (see Fig. 7, A and B). To examine its time course, we applied two depolarizing pulses (-50 mV to +80 mV) in succession, and varied the interval between the two pulses (Fig. 8A). For each pair of pulses, the charge moved (Q_{ON}) for the second pulse (Q_2) was normalized with respect to that of the first pulse (Q_1). The charge for the second pulse decreased exponentially as the interval between the two pulses was shortened (Fig. 8B). The time constant for the recovery of charge ($\tau_{Recovery}$) was 516 ± 65 ms ($N = 4$) (Fig. 8B). $\tau_{Recovery}$ was independent of the test voltage (Fig. 8C).

Thus, GAT4 voltage-induced presteady-state currents resemble those previously reported for mGAT3, however, they exhibit significantly slower kinetics (Sacher et al., 2002). The slow recovery of charge from a depolarizing voltage has been proposed to represent the rate-limiting step(s) in the transport cycle. These steps are thought to represent conformational changes of the empty carrier, Na^+ entry into the membrane electric field, Na^+ binding,

and binding-induced conformational changes (see Fig. 12B) (Mager et al., 1993, 1996; Lu & Hilgemann, 1999b; Li et al., 2000; Sacher et al., 2002). If these steps are taken to represent the rate-limiting steps in the transport cycle, the time constant of charge recovery (516 ms; Fig. 8B) predicts a transport cycle turnover rate of 1.9 s^{-1} (see also Figs.10 and 11B).

Na^+-, Cl^-, AND GABA-DEPENDENCE OF PRESTEADY-STATE CHARGE MOVEMENTS

Reduction in $[Na^+]_o$ led to a decrease in Q_{max}, and at nominal zero $[Na^+]_o$ (106 mM Cl^- present), Q_{max} was below the resolution of the measurements (≈ 2 nC) (Fig. 9A). The increase in Q_{max} as a function of $[Na^+]_o$ followed a sigmoidal relationship with a half-maximal concentration of 50 ± 2 mM, and a Hill coefficient of 3.0 ± 0.6 ($N = 3$) (Fig. 9A). Similar to that seen for other Na^+-coupled transporters, a 10-fold reduction in $[Na^+]_o$ shifted the $V_{0.5}$ of the Q-V relationship as well as the peak of the τ_{ON}-V relationship toward negative membrane potentials by ~100 mV (not shown; see Hazama et al., 1997; Sacher et al., 2002). As $[Na^+]_o$ was reduced, the presteady-state current relaxations became faster, while the apparent valence of the moveable charge ($z\delta$) was not altered (not shown).

The strong Cl^- dependence of the steady-state characteristics (see Fig. 1, A and D, and Fig. 2C) prompted us to examine the Cl^- dependence of the voltage-induced presteady-state charge movements (Fig. 9B). Reductions in $[Cl^-]_o$ led to decreases in Q_{max}. However, the presteady-state charge movements were not absolutely dependent on Cl^-, as significant charge movements were observed at nominal zero $[Cl^-]_o$; Q_{max} was 25 ± 3% of that at 106 mM Cl^- ($N = 4$) (Fig. 9B). Cl^--enhancement of charge movements appeared to be saturable; however, its half-maximal concentration and Hill coefficient could not be determined due to its low apparent affinity (≥100 mM) (Fig. 9B). As $[Cl^-]_o$ was reduced from 106 mM to 0 mM ($[Na^+]_o = 100$ mM): (i) the $V_{0.5}$ of the Q-V relationship shifted toward negative membrane potentials by ~50 mV, (ii) the presteady-state current relaxations became faster, and (iii) the apparent valence of the moveable charge ($z\delta$) was not altered (not shown).

Saturating concentrations of GABA led to complete abolition of the presteady-state currents (Fig. 9C). The GABA concentration for 50% reduction in Q_{max} was 7 ± 1 μM ($N = 3$). $V_{0.5}$, $z\delta$, and the relaxation time constants were not significantly altered by GABA (not shown). Flufenamic acid also led to the inhibition of the presteady-state charge movements (Fig. 9D). The flufenamic acid concentration for 50% reduction in Q_{max} was 442 ± 30 μM ($N = 3$) (Fig. 9D). This is significantly greater than the concentration needed for 50% inhibition of $Na^+/$
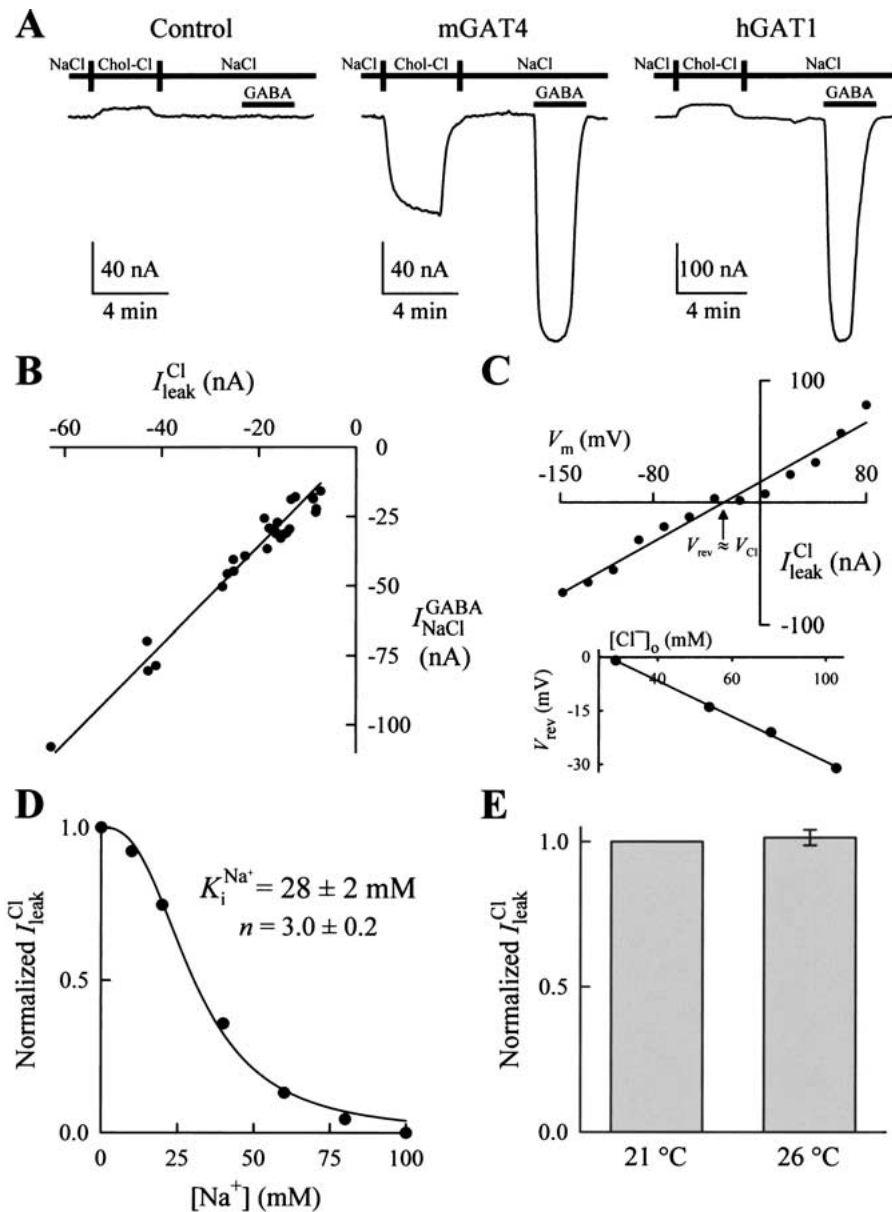
Fig. 4. GAT4 exhibits a Na^+-inhibited Cl^- leak conductance. (A) In cells expressing GAT4, removal of Na^+ from the bath (choline or TEA replacement) led to an inward current (*middle trace*) ($V_m = -60$ mV). The current was present in the absence of GABA and was not altered by addition of GABA. Therefore, the current represents an uncoupled (or leak) mode of the transporter. This leak current is carried by Cl^- ions and, thus, it is referred to as I_{leak}^{Cl}. I_{leak}^{Cl} was not observed in control cells or hGAT1-expressing cells (*left* and *right traces*). (B) When examined in the same cells, I_{leak}^{Cl} was directly proportional to the GABA-evoked inward current (I_{NaCl}^{GABA}). At -60 mV, I_{leak}^{Cl} was $55 \pm 4\%$ of I_{NaCl}^{GABA} ($N = 29$). (C) I_{leak}^{Cl} reversed at the calculated Cl^- equilibrium potential. The current-voltage relationship (-150 to $+80$ mV) was obtained by sub-

tracting current values in the presence of NaCl from corresponding values in the presence of choline-Cl. Similar I-V relationships were obtained when values in the presence of choline-Cl and flufenamic acid (500 μM) were subtracted from those obtained in the presence of choline-Cl (*see* Fig. 6). The reversal potential (V_{rev}) for I_{leak}^{Cl} closely followed the predicted Cl^- Nernst potential (V_{Cl}); the slope was 56 ± 3 mV/decade ($N = 4$). (D) Na^+ led to a concentration-dependent inhibition of I_{leak}^{Cl}; the Na^+ concentration for 50% inhibition was 28 ± 2 mM, and the Hill coefficient was 3.0 ± 0.2 ($N = 4$) ($V_m = -80$ mV). (E) I_{leak}^{Cl} was temperature-independent. The Q_{10} (21–26°C) was 1.03 ± 0.01 ($N = 3$). The measurements were taken at $V_m = -80$ mV.

Cl^-/GABA cotransport and the Na^+-inhibited leak modes of conduction (≈30 μM). As the voltage-induced charge movements of GAT4 are most pro-

nounced at positive voltages ($V_{0.5} \approx 20$ mV; *see* Fig. 7C), it is possible that the interaction of flufenamic acid with GAT4 is voltage-dependent; i.e.,
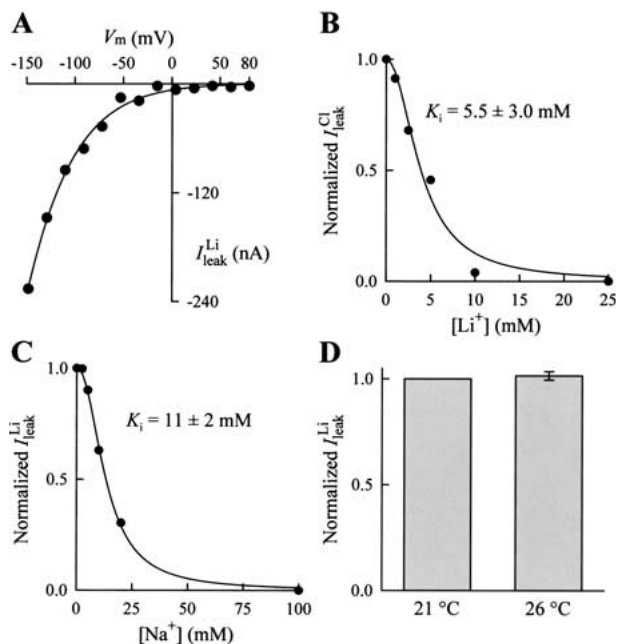
Fig. 5. GAT4 exhibits a Na^+-inhibited Li^+ leak conductance. (*A*) In cells expressing GAT4, replacement of external Na^+ with Li^+ caused a Li^+ leak current. This current will be referred to as I_{leak}^{Li}. The current-voltage relationship (-150 to $+80$ mV) was obtained by subtracting current values in the presence of NaCl from corresponding values in the presence of LiCl. The Li^+ leak current was most pronounced at hyperpolarized potentials, and approached zero at depolarized potentials. (*B*) Li^+ inhibited the Cl^- leak current (I_{leak}^{Cl}) in a concentration-dependent manner. At $+80$ mV (a voltage at which no I_{leak}^{Li} is present; *see* panel *A*), the Li^+ concentration for 50% inhibition of I_{leak}^{Cl} was 5.5 ± 3.0 mM, and the Hill coefficient was 1.5 ± 0.2 ($N = 4$). (*C*) Na^+ led to a concentration-dependent inhibition of I_{leak}^{Li}. The Na^+ concentration for 50% inhibition of I_{leak}^{Li} was 11 ± 2 mM, and the Hill coefficient was 1.8 ± 0.3 ($N = 3$) ($V_m = -80$ mV). (*D*) I_{leak}^{Li} was temperature independent. The Q_{10} ($21–26°C$) was 1.01 ± 0.03 ($N = 4$). The measurements were taken at $V_m = -80$ mV.
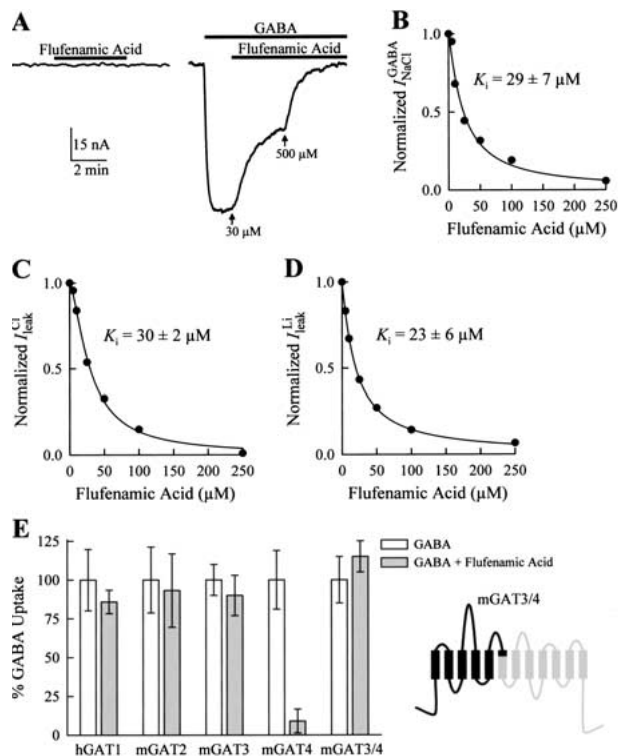
Fig. 6. Isoform-specific inhibition of GAT4 by flufenamic acid. (*A*) Application of flufenamic acid (500 μM) to GAT4-expressing cells did not alter the holding current (*left trace*) ($V_m = -60$ mV). When applied in the presence of GABA, however, flufenamic acid led to the inhibition of GAT4 Na^+/Cl^-/GABA cotransport across the plasma membrane (*right trace*). (*B*) The flufenamic acid concentration for 50% inhibition of the GABA-evoked current (I_{NaCl}^{GABA}) was 29 ± 7 μM ($N = 5$). [GABA] was 200 μM. (*C* and *D*) flufenamic acid also inhibited I_{leak}^{Cl} ($K_i = 30 \pm 2$ μM; $N = 3$) (*C*) and I_{leak}^{Li} ($K_i = 23 \pm 6$ μM; $N = 3$) (*D*). (*E*) Flufenamic acid (500 μM) inhibited only GAT4-mediated [^{3}H]-GABA uptake, and had no significant effect on GABA transport mediated by hGAT1, mGAT2, mGAT3, or a chimeric GAT3/4 protein ($P > 0.1$). The data for each bar represent the mean $\pm$ SE from ≥15 cells. Similar results were obtained with cells from three donor frogs. *Inset* shows the predicted topology of the chimeric mGAT3/4 protein, in which the black region corresponds to the amino half of mGAT3, and the gray region corresponds to the carboxy half of mGAT4 (*see* Materials and Methods).

membrane depolarization may reduce the apparent affinity of GAT4 for flufenamic acid.

Thus, the voltage-induced charge movements are strictly dependent on external Na^+, they are enhanced by external Cl^-, and they are completely abolished in the presence of saturating concentrations of GABA and/or inhibitor (Fig. 9). These features are depicted in a simple kinetic scheme proposed in Fig. 12 (*see* Discussion).

GAT4 Steady-State Turnover Rate

Q_{max} is a measure of the total number of functional transporters in the plasma membrane (Eskandari et al., 2000), and I_{max} represents the maximum rate of GABA transport across the plasma membrane (*see* Fig. 1*C*). Thus, the turnover rate (R_{TO}) of GAT4 was estimated according to $R_{TO} = I_{max}/Q_{max}$ (Mager

et al., 1993; Eskandari et al., 1997; Sacher et al., 2002). In a group of oocytes, both Q_{max} and I_{max} were measured. In each oocyte, Q_{max} was measured (*see* Fig. 7) and, subsequently, I_{max} was measured at 1 mM GABA. The slope of the plot I_{max} *vs.* Q_{max} provided an estimate of the turnover rate of GAT4 (Fig. 10). The GAT4 turnover rate was 1.5 ± 0.1 s^{-1} at -50 mV and 21°C ($N = 27$). The temperature dependence of the cotransport cycle ($Q_{10} = 4.3$; *see* Fig. 3) suggests that at 37°C and -50 mV, the GAT4 turnover rate is 15.5 s^{-1}. The GAT4 *I-V* relationship (Fig. 1*D*) predicts a turnover rate of 20 s^{-1} at -90 mV.

A

700 nA

200 ms

B

mV
+80
+70
+60
+50
+40
+30
+20
+10
0

400 nA

200 ms

C

Q_{ON} (nC)

65

30

-70   -40   0   40   80

V_m (mV)

D

τ_{ON} (ms)
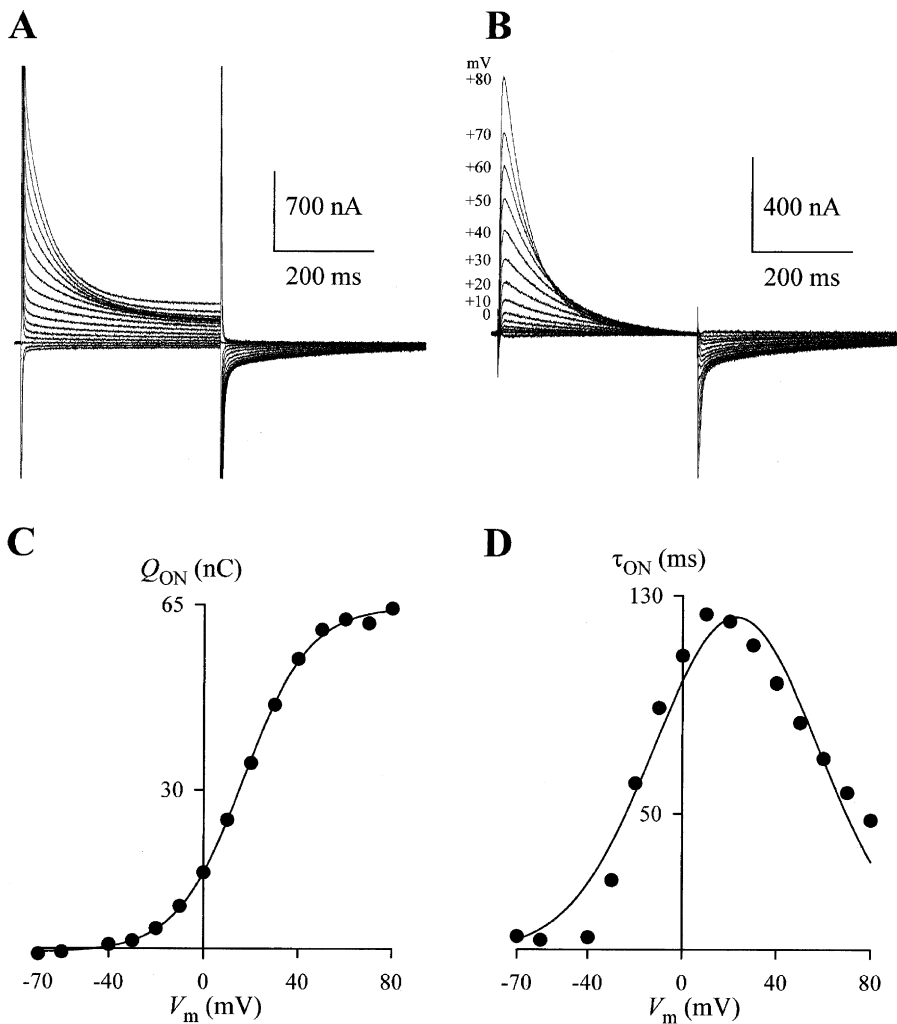
130

50

-70   -40   0   40   80

V_m (mV)

Fig. 7. Presteady-state charge movements of GAT4. (*A*) Step changes in the membrane potential of GAT4-expressing cells evoked presteady-state current transients. The holding potential was −50 mV, and the voltage pulses (400 ms) ranged from +80 mV to −70 mV in 10-mV steps. These transients were not observed in control cells (*not shown*). Notice that the OFF transients relaxed very slowly to a steady-state (*see* text and Fig. 8). (*B*) The charge movements were isolated after subtraction of the records in the absence of Na^+ (choline replacement) (Sacher et al., 2002). (*C*) At each applied voltage, time integration of the ON transients in panel *B* yielded the charge moved. The charge-voltage (*Q-V*) relationship obtained was fitted to a single Boltzmann function (Eq. 3). The parameters obtained from the fit were: $V_{0.5}$, 18 ± 1 mV and $z\delta$, 1.8 ± 0.1 ($N = 26$). The maximum charge (Q_{max}) depended on GAT4 expression at the cell surface (*see* Fig. 10). (*D*) The GAT4 ON transients exhibited mono-exponential relaxation. The time constant of the relaxation (τ_{ON}) as a function of the test voltage (τ_{ON} -*V* relationship) followed a bell-shaped function. The voltage at maximum τ_{ON} was 21 ± 3 mV ($N = 26$). This voltage is similar to the $V_{0.5}$ of the *Q-V* relationship (panel *C*). The line is the fit of the data to a bell-shaped function (*see* Sacher et al., 2002).

RAPID CONCENTRATION JUMPS AT GAT4

To gain further insight into the nature of ion and GABA binding and translocation by GAT4, we performed concentration jump experiments (Mager et al., 1996). The slow turnover rate of GAT4 (1.5 s^{-1} at −50 mV and 21°C) makes it possible to perform concentration jumps in intact, voltage-clamped oocytes in order to gain information about partial steps of the transport cycle. The results of representative concentration jump experiments are shown in Fig. 11. In *panel A*, an oocyte expressing GAT4 was

voltage-clamped at −50 mV and was stabilized in the NaCl buffer. Rapid introduction of GABA (1 mM) into the bath evoked an inward current with three distinct phases (Fig. 11*A*): (*i*) a rapid transient phase with a time-to-peak of 20 ± 2 ms and a decay time constant of 15 ± 2 ms, (*ii*) a slower transient phase ($\tau = 1.3 \pm 0.1$ s), and (*iii*) a steady-state current ($N = 6$). Comparison of this trace with those shown in Figs. 1, 3, 4, and 6 reveals that the first and second (transient) components are missed entirely in conventional two-electrode voltage-clamp measurements. For clarity, the first and second components
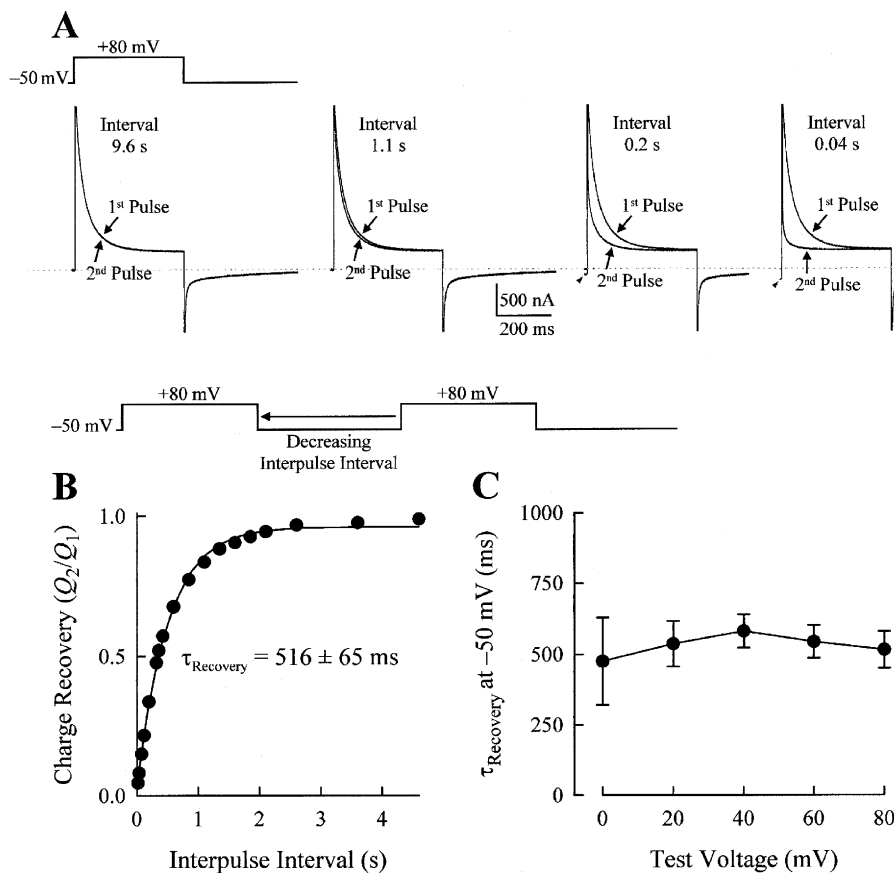
Fig. 8. Slow relaxation of presteady-state OFF transients. (*A*) Two pulses (400 ms; −50 mV to +80 mV) were applied in succession with a defined interpulse interval, and the resulting current traces were superimposed. As the interpulse interval was shortened, the presteady-state charge movements became smaller. Notice that for very short interpulse intervals, when the second pulse was applied, the OFF transients had not yet decayed back to the holding level (*arrowheads*). The *dashed line* represents the baseline holding current. For each trace, the presteady-state charge movements were extracted from the total current trace, and the charge moved was quantified (*see* panel *B*). (*B*) Two pulses were applied in succession (as in panel *A*) while the interpulse interval was varied. The charge moved in response to the second pulse (Q_2) was normalized with respect to that moved in response to the first pulse (Q_1). Charge recovery (Q_2/Q_1) plotted as function of the interpulse interval followed a single rising exponential function with a time constant ($\tau_{recovery}$) of 516 ± 65 ms ($N = 4$). (*C*) Double-pulses were applied from a holding voltage of −50 mV to test voltages ranging from 0 to 80 mV, and the interpulse interval was varied in order to determine $\tau_{recovery}$ (as shown in panel *B*). $\tau_{recovery}$ was independent of the test voltage.

are expanded in the *insets* (Fig. 11*A*, 1 and 2). Upon rapid removal of GABA from the bathing medium, return of the evoked current to the baseline followed a slow single-exponential decay with a time constant of 12.0 ± 0.6 s ($N = 6$). GABA jumps do not evoke either a transient or steady-state current in control cells (*not shown*).

In Fig. 11*B*, the oocyte was initially stabilized in a solution in which neither Na$^+$ nor GABA was present (TEA replaced Na$^+$, but Cl$^-$ was present). Rapid introduction of Na$^+$ and GABA into the bath evoked an inward current with single-exponential growth to a steady state ($\tau = 602 \pm 76$ ms; $N = 6$). The data show that preincubation of the transporter with Na$^+$ is necessary to obtain the rapid transient phases observed in Fig. 11*A*. Washout

of Na$^+$ and GABA led to rapid return of the evoked current back to the baseline ($\tau = 645 \pm 34$ ms; $N = 6$). Similar rising and decay time constants were obtained whether or not Cl$^-$ was initially present (*not shown*).

Altogether, these experiments suggest that Na$^+$ binding and subsequent conformational changes induced by Na$^+$ binding constitute the rate-limiting steps in the transport cycle (*see* Fig. 12*B*) (Hilgemann & Lu, 1999; Li et al., 2000). Moreover, the Na$^+$- and Cl$^-$-bound transporter can bind and translocate GABA very rapidly (*see* Discussion and Fig. 12). If Na$^+$ binding and induced conformational changes are taken to represent the rate-limiting steps, the activation time constant obtained from Fig. 11*B* (600 ms) suggests a cotransport turnover rate of 1.7 s^{-1}.
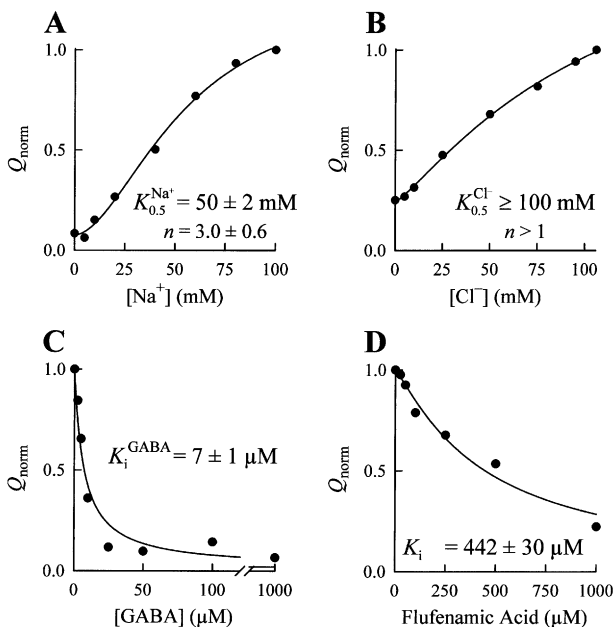
Fig. 9. Activation and inhibition of the presteady-state charge movements by ligands and inhibitor. (*A–D*) Q_{max} was quantified in the presence of increasing concentrations of the indicated ligands, and normalized (Q_{norm}) with respect to that obtained at 100 mM Na^+, 106 mM Cl^-, and in the absence of GABA or inhibitor. The presteady-state charge movements were activated by Na^+ ($K_{0.5} = 50 \pm 2$ mM; $N = 3$), enhanced by Cl^- ($K_{0.5} \geq 100$ mM; $N = 4$), and inhibited by GABA ($K_i = 7 \pm 1$ µM; $N = 3$) and flufenamic acid ($K_i = 442 \pm 30$ µM; $N = 3$). In panel *A*, $[Cl^-]$ was held constant at 106 mM. In panel *B*, $[Na^+]$ was held constant at 100 mM. In panels *C* and *D*, $[Na^+]$ was 100 mM, and $[Cl^-]$ was 106 mM.

Discussion

The present study provides evidence for the existence of Na^+-inhibited Cl^- and Li^+ leak currents in GAT4. Both leak currents appear to utilize a channel-like permeation pathway, but it is not known whether they share a common pathway. The two leak modes appear not to coexist, as Li^+ inhibits the Cl^- leak mode. Existence of a Cl^--channel mode prompted us to examine the effect of a number of Cl^--channel blockers on GAT4 function. Interestingly, flufenamic acid reversibly inhibits all functional features of GAT4 ($Na^+/Cl^-/GABA$ cotransport, Cl^- and Li^+ leak, and presteady-state charge movements), and shows little or no selectivity for GAT1, GAT2, or GAT3. We also show that the high temperature dependence of GAT4 $Na^+/Cl^-/GABA$ cotransport across the plasma membrane suggests higher than anticipated turnover rates at physiological temperatures and membrane voltages (15–20 s^{-1}). Finally, by utilizing rapid concentration jumps, we provide additional support for the notion that Na^+ binding to the transporter and associated conformational changes constitute the rate-limiting steps in $Na^+/Cl^-/$
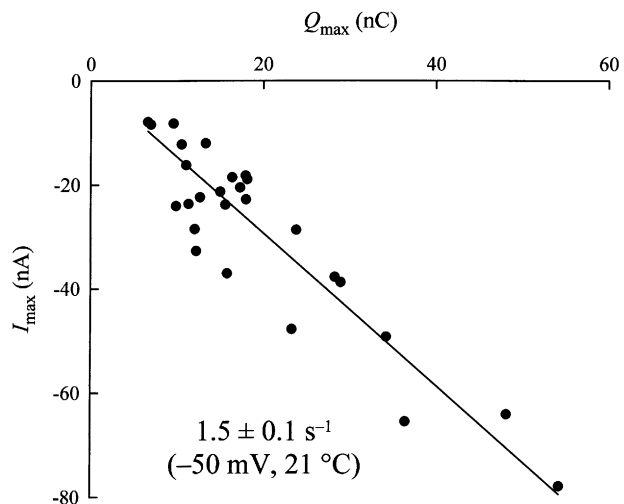

Fig. 10. Steady-state turnover rate of GAT4. The turnover rate (R_{TO}) of GAT4 was estimated according to $R_{TO} = I_{max}/Q_{max}$. In a group of GAT4-expressing cells, both Q_{max} (*see* Fig. 7) and I_{max} (at 1 mM GABA) were measured. At −50 mV and 21°C, the GAT4 turnover rate was 1.5 ± 0.1 s^{-1} ($N = 27$). Each data point corresponds to Q_{max} and I_{max} measurements from a single oocyte.

GABA cotransport across the plasma membrane. Thus, the combined rate for these steps governs the turnover rate of the entire transport cycle.

GENERAL STEADY-STATE PROPERTIES OF GAT4

The steady-state properties of GAT4 exhibit most of the features that are unique to the members of this family of transporters; however, some features differ significantly from those found in other members. The salient features are emphasized below: (*i*) GAT4 GABA transport across the plasma membrane is absolutely Na^+-dependent, but it exhibits only partial dependence on Cl^-. This is consistent with a wide range of reports on GAT1, GAT2/BGT1, and GAT3 (Clark et al, 1992; Keynan et al, 1992; Mager et al., 1993, 1996; Clark & Amara, 1994; Matskevitch et al., 1999; Loo et al., 2000; Sacher et al., 2002), as well as the related taurine, glycine, dopamine, serotonin, and creatine transporters; (*ii*) Both the Na^+-activation and Cl^--enhancement of the GABA-evoked currents and the presteady-state charge movements followed a sigmoidal relationship with Hill coefficients of ≥ 2. Cooperativity with respect to Na^+-dependence is well-established, but that for Cl^- has only been shown for human (Ruiz-Tachiquem et al., 2002) and canine BGT1 (Matskevitch et al., 1999). The results suggest that ≥ 2 Na^+ and at least 2 Cl^- ions interact with GAT4 during the transport cycle. (*iii*) The coupling ratio between charge flux and GABA flux is 2 charges/GABA, similar to that reported for GAT1 and GAT3 (Loo et al., 2000; Sacher et al., 2002; Whitlow et al., 2003). Thus, currents in excess of
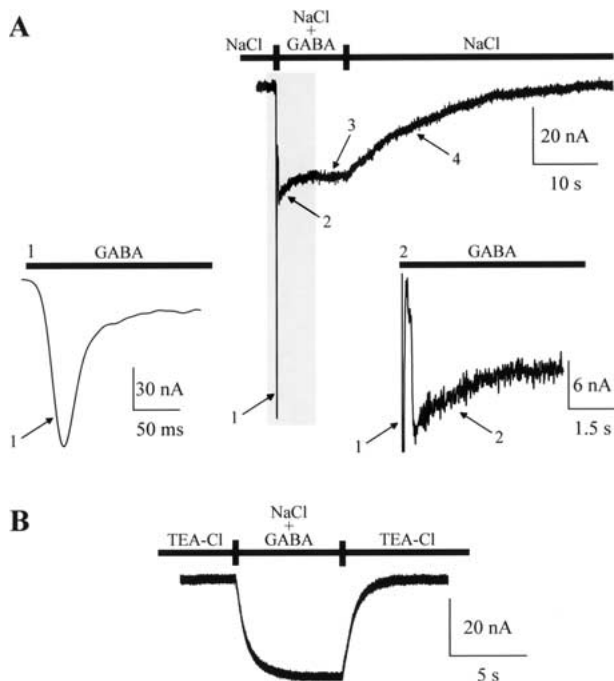
Fig. 11. Concentration jumps at GAT4. (*A*) A representative GABA concentration jump is shown (V_m = −50 mV and [GABA] = 1 mM). An oocyte expressing GAT4 was stabilized in the NaCl buffer and GABA was rapidly introduced into the bath. The GABA-evoked inward current exhibited three distinct phases; (*i*) a rapid transient current (*arrow* at 1 and expanded in *inset* 1), (*ii*) a slow transient phase (*arrow* at 2 and expanded in *inset* 2), and (*iii*) a steady-state current (*arrow* at 3). For the rapid transient phase, the time-to-peak was 20 ± 2 ms, and its decay had a time constant of 15 ± 2 ms (N = 6). The slow transient phase exhibited mono-exponential decay to a steady state with a time constant of 1.3 ± 0.1 s (N = 6). The rapid and slow transient currents are absent in the conventional two-electrode voltage-clamp records shown in Figs. 1, 3, 4, and 6. Only the steady-state current is observed in conventional two-electrode voltage-clamp records. Upon rapid removal of GABA, the GABA-evoked current exhibited mono-exponential decay (*arrow* at 4) back to the baseline with a time constant of 12.0 ± 0.6 s (N = 6). (*B*) The oocyte was stabilized in a Na^+-free buffer (equimolar replacement of NaCl with TEA-Cl), followed by rapid introduction of Na^+ (100 mM) and GABA (1 mM) into the bath. The evoked current followed single exponential growth to a steady state with a time constant of 602 ± 76 ms (N = 6). Upon removal of Na^+ and GABA, the evoked current decayed back to the baseline with a time constant of 645 ± 34 ms (N = 6).

GABA flux are not observed, suggesting that under these conditions the transport coupling stoichiometry is similar to that of GAT1; 2 Na^+:1 Cl^-:1 GABA per transport cycle (Pastuszko, Wilson & Erecinska, 1982; Radian & Kanner, 1983; Lu & Hilgemann, 1999a; Loo et al., 2000). (*iv*) The turnover rate of GAT4 (1.5 s^{-1} at 21°C and −50 mV) is lower than that reported for GAT1 (6 s^{-1}), GAT2/BGT1 (10 s^{-1}), and GAT3 (1.7 s^{-1}) (Mager et al., 1993; Forlani et al., 2001; Sacher et al., 2002). (*v*) Na^+/Cl^-/GABA cotransport across the plasma membrane is highly

temperature-dependent with an activation energy of 29 ± 1 kcal/mol (16–31°C) and a Q_{10} of 4.3 (21–31°C). This is significantly higher than that reported for GAT1 (Q_{10} = 2.2) (Binda et al., 2002). The Q_{10} predicts a turnover rate of 15.5 s^{-1} at −50 mV and 37°C. Moreover, given that GAT4 is predominantly expressed in astrocytes (Itouji et al., 1996; Minelli et al., 1996; Gadea & López-Colomé, 2001; Conti et al., 2004), and that physiological astrocytic membrane potential is −80 to −90 mV (Kinney & Spain, 2002), the GAT4 *I-V* relationship (*see* Fig. 1*D*) predicts a physiological turnover rate of ≈20 s^{-1}. As the predicted physiological turnover rate is still too slow for effective attenuation of synaptic GABA concentration (one transport cycle lasts 50–67 ms), we speculate that GAT4 must be expressed at high levels at or around synaptic regions, as has been shown for GAT1 (~1,000 per μm^2) (Chiu et al., 2002). Thus, GABA binding and rapid translocation may serve as the first steps in "buffering" synaptically released GABA (see Fig. 12*D*) (Lester, Cao & Mager, 1996; Hilgemann & Lu, 1999).

GAT4 Cl^- AND Li^+ LEAK CURRENTS APPEAR TO BE MEDIATED BY CHANNEL MODES OF THE TRANSPORTER

Uncoupled or leak currents have been observed in a number of electrogenic Na^+-coupled transporters from different gene families (Senders & Amara, 1996; Wright et al., 1996; Forster et al., 2002; DeFelice, 2004). These currents may be present in the absence of substrate, or they may be activated by the transporter substrate. For example, in the absence of substrate, the Na^+/iodide, Na^+/phosphate, and Na^+/glucose cotransporters function as Na^+ uniporters (Wright et al., 1996; Eskandari et al., 1997; Forster et al., 2002), whereas the glutamate transporters may also be thought of as glutamate-gated Cl^- channels (Fairman et al., 1995). In some transporters, the uncoupled currents are thought to result from channel modes of activity (e.g., glutamate, dopamine, norepinephrine, and serotonin transporters) (Fairman et al., 1995; Galli, Blakely & DeFelice, 1996; Lin, Lester & Mager, 1996; Sonders & Amara, 1996; Galli et al., 1997; Sonders et al., 1997; DeFelice, 2004), whereas in others, they are thought to be manifestations of transporter conformational changes (e.g., Na^+/glucose cotransporter) (Panayotova-Heiermann et al., 1998).

In the Na^+/Cl^-/GABA cotransport mode of function, the GABA transporters exhibit a fixed stoichiometry of 2 Na^+:1 Cl^-:1 GABA per transport cycle. Thus, currents in excess of substrate fluxes are not observed for the GABA transporters (*see* Fig. 1*C*) (Loo et al., 2000; Sacher et al., 2002; Whitlow et al., 2003). Thus, substrate and ion fluxes appear to be tightly coupled in the GABA transporters.
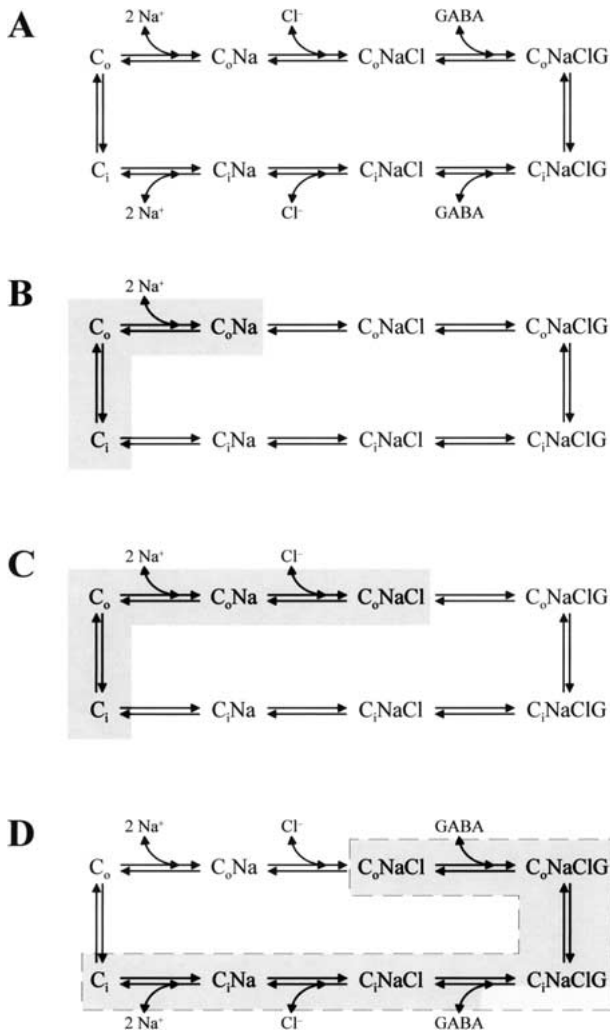
Fig. 12. Kinetic scheme of GAT4 transport cycle. Kinetic representation of the minimal steps required to describe GABA transporter function (Nelson, 1998; Hilgemann & Lu, 1999; Sacher et al., 2002). C denotes carrier; Na, Na^+; Cl, Cl^-; and G, GABA. The subscripts "o" and "i" refer to the outward- and inward-facing carrier binding sites. (*A*) Clockwise transitions of the entire transport cycle result in forward $Na^+/Cl^-/GABA$ cotransport into the cell. (*B–D*) Voltage-induced charge movements are seen upon application of voltage pulses in the presence of Na^+ (*B*), they are enhanced by Cl^- (*C*), and they are completely abolished by saturating concentrations of GABA (*D*) or inhibitor. The *shaded regions* in panels *B* and *C* represent the transitions that are thought to be induced by voltage pulses, and likely are responsible for the presteady-state charge movements (counterclockwise transitions). By enhancing the maximum charge moved, Cl^- appears to stabilize the Na^+-loaded state of the transporter (*see* text and Sacher et al., 2002). (*D*) Binding of GABA to the Na^+- and Cl^--loaded carrier induces rapid conformational changes that result in introduction of net charge into the cytoplasm (*shaded* steps enclosed by *dashed line* panel *D*). The *shaded* steps in *panel D* (clockwise transitions) may be responsible for the rapid transient observed with GABA concentration jumps (Fig. 11*A*). The rate-limiting steps for the entire transport cycle appear to be those shaded in panel *B* (clockwise transitions). *See* text for additional details.

This behavior is similar to that seen for the related glycine transporter (Roux & Supplisson, 2000), but in contrast to that seen for the related norepinephrine, dopamine, and serotonin transporters (Galli et al., 1997; Senders et al., 1997; Quick, 2003).

The only well-documented uncoupled current observed for the GABA transporters is a Na^+-inhibited Li^+ leak current (I_{leak}^{Li}), which has been attributed to a channel mode of transporter function (Mager et al., 1996; Bismuth et al., 1997; MacAulay et al., 2002; Grossman & Nelson, 2003; Kanner, 2003). In GAT1, the Li^+ leak is inhibited by Na^+ (MacAulay et al., 2002; Kanner, 2003), but it is enhanced by Cl^- (Mager et al., 1996; Bismuth et al., 1997). The leak pathway also allows the permeation of cesium and potassium (Mager et al, 1996; Kanner, 2003). The properties of GAT4 I_{leak}^{Li} observed here are in agreement with those reported for GAT1. The lack of temperature dependence observed for GAT4 I_{leak}^{Li} supports the view that the Li^+ leak is mediated by a channel mode of the transporter (MacAulay et al., 2002). A Li^+ leak has also been documented for the related serotonin and dopamine transporters (Mager et al., 1994; Senders et al., 1997). In GAT4, GABA does not alter the lithium leak, presumably because of its lack of interaction with the transporter in the absence of Na^+. Serotonin, however, abolishes the Li^+ leak of the serotonin transporter in the absence of Na^+, suggesting that serotonin can bind to its transporter in the absence of Na^+ (Mager et al., 1994). A similar picture has been shown for the dopamine transporter (Senders et al., 1997).

Here, we show that in addition to the Li^+ leak, GAT4 exhibits a novel Cl^- leak current (I_{leak}^{Cl}). Our results suggest that I_{leak}^{Cl} is a Na^+-inhibited Cl^- current conducted by a channel-like permeation pathway within GAT4. Three observations support this conclusion: (*i*) Na^+ leads to a concentration-dependent reduction in I_{leak}^{Cl}, (*ii*) I_{leak}^{Cl} reverses at the Cl^- equilibrium potential, and (*iii*) I_{leak}^{Cl} is not temperature-dependent ($Q_{10} \approx 1$). At present, it is not known whether the Cl^- recognition site is the same as that used in the cotransport mode. The small magnitude of I_{leak}^{Cl} suggests that the single-channel conductance (γ) and/or the open-state probability (P_o) are very small. Based on the magnitude of I_{leak}^{Cl} relative to the GABA-evoked current (*see* Fig. 4*B*), and the correlation between the GABA-evoked current and transporter surface expression (*see* Fig. 10), the product of the single-channel conductance and open-state probability ($P_o\gamma$) is estimated to be $\sim 1 \times 10^{-17}$.

At least four observations suggest that the Cl^- leak conductance is not significant in the presence of Na^+ (≥ 100 mM), either in the absence of GABA or during the $Na^+/Cl^-/GABA$ cotransport cycle: (*i*) I_{leak}^{Cl} is inhibited by Na^+ ($K_i = 28$ mM) in a highly cooperative fashion (Hill coefficient of 3), such that at 100 mM Na^+, nearly 100% of I_{leak}^{Cl} is inhibited; (*ii*)

while flufenamic acid completely blocks I_{leak}^{Cl} in the absence of Na^+ (Fig. 6C), in the presence of Na^+ (GABA absent), no residual leak current is blocked by this agent (Fig. 6A); (iii) while the cotransport cycle is highly temperature-dependent (Q_{10} = 4.3), I_{leak}^{Cl} is temperature-independent ($Q_{10} \approx 1$); i.e., significant contribution of I_{leak}^{Cl} to the cotransport current is expected to lower the temperature dependence of the GABA-evoked current; and (iv) in the cotransport mode of function, GABA flux is directly proportional to charge flux into the cell. Since currents in excess of fluxes are not observed, when coupled to GABA translocation, Na^+ and Cl^- permeation through GAT4 appears to be strictly coupled to transporter conformational changes (Hilgemann & Lu, 1999).

These results suggest that, in the absence of Na^+, two leak pathways exist in GAT4: a Cl^- permeation pathway and a Li^+ permeation pathway. Both conduction pathways appear channel-like, although it is not known whether the two leak modes share a common permeation pathway. If Na^+ is replaced with a large cation such as choline or tetraethylammonium (cations that do not interact with the transporter), GAT4 assumes a conformation that favors a Cl^- channel mode of the transporter. Binding of Na^+ to the transporter occludes the Cl^- permeation pathway and prepares the transporter for GABA binding. If Na^+ is replaced with Li^+, a Li^+ leak is observed, which is favored at hyperpolarized membrane voltages. Li^+ binding to the transporter appears to occlude the Cl^- permeation pathway. Lithium blockade of the Cl^- leak most likely occurs via a Li^+ binding-induced conformational change of the transporter rather than a physical block of the Cl^- permeation pathway by Li^+. In contrast, Cl^- binding to the transporter enhances the Li^+ leak (Mager et al., 1996; Bismuth et al, 1997). Remarkably, binding of Na^+ occludes both channel modes and prepares the transporter for GABA binding. As the leak modes do not exist at high Na^+ concentrations, the physiological implications of the leak modes are not clear.

Isoform-Specific Inhibition of GAT4

Given the functional differences between the GABA transporter isoforms, and their differential localization within the central nervous system, it is of considerable interest to develop/discover isoform-specific inhibitors. However, specific and high-affinity inhibitors exist only for GAT1. Tiagabine, SKF 89976-A, NO−711, and Cl−966, are all high-affinity inhibitors of GAT1 with little or no selectivity for the other isoforms (GAT2, GAT3, and GAT4) (Borden, 1996; Krogsgaard-Larsen et al, 2000; Dalby, 2003). SNAP 5114, a high-affinity inhibitor of GAT4 (K_i = 5 µM) also inhibits GAT3 (K_i = 21 µM), GAT2 (K_i = 140

µM), and GAT1 (K_i = 388 µM) (Borden et al., 1994). Here, we have shown that the chloride-channel blocker, flufenamic acid, inhibits all functional features of GAT4, and that it exhibits little or no selectivity for GAT1, GAT2, or GAT3. Flufenamic acid is effective in inhibiting Na^+/Cl^-/GABA cotransport, the Cl^- and Li^+ leak modes, as well as transporter presteady-state charge movements. As flufenamic acid can inhibit GAT4 features in the presence or absence of Na^+ and/or GABA, this agent most likely does not interact at the Na^+ or GABA binding site. Because flufenamic acid inhibits the leak and cotransport modes with the same potency, the results hint at the possibility that the leak and cotransport modes of the transporter share a common permeation pathway.

Flufenamic acid should be of value in synaptic and cell physiological studies that examine the contribution of GAT4 to a Na^+-dependent, GABA-evoked current. As GAT1 and GAT4 are co-expressed in various brain regions (Borden, 1996; Gadea & López-Colomé, 2001; Conti et al., 2004), the use of flufenamic acid alone or in combination with a specific GAT1 inhibitor (e.g., SKF 89976-A or NO−711) will undoubtedly reveal novel insight into the role played by GAT4 in shaping synaptic and extra-synaptic GABAergic neurotransmission. Moreover, flufenamic acid may now serve as a lead compound in structure-guided design of GAT4-specific drugs.

Voltage- and Ligand-Induced Presteady-State Transients

A great deal has been learned about the rapid kinetics of electrogenic Na^+-coupled cotransporters. This knowledge has come primarily from the use of transmembrane voltage jumps (Loo et al., 1993; Mager et al., 1993, 1996; Wadiche et al., 1995; Eskandari et al., 1997; Hazama et al., 1997; Lu & Hilgemann, 1999b; Li et al., 2000; Loo et al., 2000; Forster et al., 2002; Sacher et al., 2002; Whitlow et al., 2003), as well as voltage jumps combined with optical measurements (Li et al., 2000). The voltage-induced presteady-state currents are present in the absence of GABA and are thought to result from partial reactions of the transport cycle (Fig. 12). Upon application of depolarizing voltage pulses, the ON transients are thought to represent the release of Na^+ and Cl^- followed by reorientation of the empty carrier (shaded steps in Fig. 12C). Upon return from depolarizing voltage pulses to the holding voltage, the OFF transients represent the return of the binding sites to the external medium, Na^+ and Cl^- entry into the membrane electric field, binding, and subsequent ligand-induced conformational changes (Fig. 12C) (Loo et al., 1993; Mager et al., 1993, 1996; Hilgemann & Lu, 1999; Lu & Hilgemann, 1999a, b; Li et al.,

2000; Sacher et al., 2002). The OFF transients of GAT4 are significantly slower than the ON transients and appear to represent the rate-limiting steps in the transport cycle (*see* below). The presteady-state charge movements are strictly dependent on Na^+, and are enhanced by Cl^-. Reducing the Na^+ or Cl^- concentration leads to a reduction in Q_{max} and a shift of the charge-voltage (*Q-V*) relationship toward negative membrane potentials. However, based strictly on the ionic nature, opposite effects of Na^+ and Cl^- are expected. The strict dependence of the charge movements on Na^+ suggests that Cl^- itself does not contribute to the charge moved by the transporter, but rather Cl^- binding to the transporter stabilizes the Na^+-loaded state (Fig. 12*C*) (Loo et al., 2000; Sacher et al., 2002).

In comparison, little is known regarding fast ligand binding events in Na^+-coupled transporters (Cammack et al., 1994; Mager et al., 1996; Lu & Hilgemann, 1999a; Grewer et al., 2000; Otis & Kavanaugh, 2000; Watzke, Bamberg & Grewer, 2001). Here, we show that rapid application of GABA to the transporter evokes an inward current with three components: (*i*) a fast transient current, (*ii*) a slower transient current, and (*iii*) a steady-state current (Fig. 11). At least two different scenarios can account for the fast GABA-evoked transient current. The first possibility is derived from a similar substrate-evoked transient current observed for the glutamate transporter (Grewer et al., 2000; Otis & Kavanaugh, 2000; Watzke et al., 2001), and may be interpreted as a transient ionic current generated by intramolecular transitions that make up half of the transport cycle (*see* Fig. 12*D*). Alternatively, the fast GABA-evoked transient current may result from transient occupancy of the transporter in the fully Na^+- and Cl^--bound state (C_oNaCl in Fig. 12) before GABA binding and translocation. These transitions are expected to be driven according to the law of mass action, and the resulting current is expected to be a capacitive current. Efforts to distinguish between the two scenarios are currently under way. Interestingly, although the fast GABA-evoked transients are observed for the forward operation of the transporter (this study; Cammack et al., 1994), they are not observed for the reverse mode (Lu & Hilgemann, 1999a). It is possible that significant asymmetry exists for the rates of the forward and reverse modes of the transporter. Importantly, the GABA-evoked transient is absent if the transporter is not preincubated with Na^+, suggesting that Na^+ binding and associated conformational changes constitute the rate-limiting steps in the transport cycle.

RATE-LIMITING STEPS IN THE TRANSPORT CYCLE

The maximum steady-state current measurements (I_{max}) plotted as a function of Q_{max}, suggested that

the turnover rate for the entire transport cycle is 1.5 s^{-1} (Fig. 10). The presteady-state OFF transient has a time constant of 516 ms (Fig. 8*B*). These transients are thought to represent conformational changes of the empty carrier, Na^+ binding to the transporter and binding-associated conformational changes. If we assume that these transitions constitute the rate-limiting step(s), the rate predicted from the relaxation of the OFF transients (1.9 s^{-1}) is in general agreement with the turnover rate determined above. In addition, the time constant for Na^+ activation of Na^+/Cl^-/GABA cotransport across the plasma membrane was 600 ms (Fig. 11*B*), suggesting a rate constant (or turnover rate) of 1.7 s^{-1}. Altogether, the data suggest that Na^+ binding to the transporter and associated conformational changes constitute the rate-limiting steps. In addition, relaxation of the presteady-state OFF transients provides a good estimate of the rate of Na^+ interaction with the transporter. Thus, the concentration-jump experiments further support the view that Na^+ binding and subsequent conformational changes must occur before GABA binding and translocation (Mager et al., 1993, 1996; Cammack et al., 1994; Lester et al., 1996; Hilgemann & Lu, 1999).

References

Binda, F., Bossi, E., Giovannardi, S., Forlani, G., Peres, A. 2002. Temperature effects on the presteady-state and transport-associated currents of GABA cotransporter rGAT1. *FEBS Lett.* **512:**303–307

Bismuth, Y., Kavanaugh, M.P., Kanner, B.I. 1997. Tyrosine 140 of the γ-aminobutyric acid transporter GAT–1 plays a critical role in neurotransmitter recognition. *J. Biol. Chem.* **272:**16096–16102

Borden, L.A. 1996. GABA transporter heterogeneity: Pharmacology and cellular localization. *Neurochem. Int.* **29:**335–356

Borden, L.A., Dhar, T.G., Smith, K., Branchek, T.A., Gluchowshi, C., Weinshank, R. 1994. Cloning of the human homologue of the GABA transporter GAT-3 and identification of a novel inhibitor with selectivity for this site. *Receptors Channels* **2:**207–312

Cammack, J.N., Rakhilin, S.V., Schwartz, E.A. 1994. A GABA transporter operates asymmetrically and with variable stoichiometry. *Neuron* **13:**949–960

Chen, N.H., Reith, M.E., Quick, M.W. 2004. Synaptic uptake and beyond: The sodium- and chloride-dependent neurotransmitter transporter family SLC6. *Pfluegers Arch.* **447:**519–531

Chiu, C.S., Jensen, K., Sokolova, I., Wang, D., Li, M., Deshpande, P., Davidson., N., Mody, I., Quick, M.W., Quake, S.R., Lester, H.A. 2002. Number, density, and surface/cytoplasmic distribution of GABA transporters at presynaptic structures of knock-in mice carrying GABA transporter subtype 1-green fluorescent protein fusions. *J. Neurosci.* **22:**10251–10266

Clark, J.A., Amara, S.G. 1994. Stable expression of a neuronal γ-aminobutyric acid transporter, GAT-3, in mammalian cells

demonstrates unique pharmacological properties and ion dependence. *Mol. Pharmacol.* **46:**550–557

Clark, J.A., Deutch, A.Y., Gallipoli, P.Z., Amara, S.G. 1992. Functional expression and CNS distribution of a β-alanine-sensitive neuronal GABA transporter. *Neuron* **9:**337–348

Conti, F., Minelli, A., Melone, M. 2004. GABA transporters in the mammalian cerebral cortex: Localization, development and pathological implications. *Brain Res. Brain Res. Rev.* **45:**196–212

Cooper, G.J., Fong, P. 2003. Relationship between intracellular pH and chloride in *Xenopus* oocytes expressing the chloride channel C1C-0. *Am. J. Physiol.* **284:**C331–C338

Dalby, N.O. 2003. Inhibition of γ-aminobutyric acid uptake: Anatomy, physiology and effects against epileptic seizures. *Eur. J. Pharmacol.* **479:**127–137

DeFelice, L.J. 2004. Transporter structure and mechanism. *Trends Neurosci.* **27:**352–359

Deken, S.L., Beckman, M.L., Boos, L., Quick, M.W. 2000. Transport rates of GABA transporters: Regulation by the N-terminal domain and syntaxin 1A. *Nat. Neurosci.* **3:**998–1003

Fesce, R., Giovannardi, S., Binda, F., Bossi, E., Peres, A. 2002. The relation between charge movement and transport-associated currents in the rat GABA cotransporter rGAT1. *J. Physiol.* **545:**739–750

Eskandari, S., Kreman, M., Kavanaugh, M.P., Wright, E.M., Zampighi, G.A. 2000. Pentameric assembly of a neuronal glutamate transporter. *Proc. Natl. Acad. Sci. USA* **97:**8641–8646

Eskandari, S., Loo, D.D.F., Dai, G., Levy, O., Wright, E.M., Carrasco, N. 1997. Thyroid Na^+/I^- symporter. Mechanism, stoichiometry, and specificity. J. Biol. Chem. **272:**27230–27238

Fairman, W.A., Vandenberg, R.J., Arriza, J.L., Kavanaugh, M.P., Amara, S.G. 1995. An excitatory amino-acid transporter with properties of a ligand-gated chloride channel. *Nature* **375:**599–603

Forlani, G., Bossi, E., Perego, C., Giovannardi, S., Peres, A. 2001. Three kinds of currents in the canine betaine-GABA transporter BGT-1 expressed in *Xenopus laevis* oocytes. *Biochim. Biophys. Acta* **1538:**172–180

Forster, I.C., Kohler, K., Biber, J., Murer, H. 2002. Forging the link between structure and function of electrogenic cotransporters: The renal type IIa Na^+/P_i cotransporter as a case study. *Prog. Biophys. Mol Biol.* **80:**69–108

Gadea, A., López-Colomé, A.M. 2001. Glial transporters for glutamate, glycine, and GABA: II. *GABA transporters. J. Neurosci. Res.* **63:**461–468

Galli, A., Blakely, R.D., DeFelice, L.J. 1996. Norepinephrine transporters have channel modes of conduction. *Proc. Natl. Acad. Sci. USA* **93:**8671–8676

Galli, A., Petersen, C.I., deBlaquiere, M., Blakely, R.D., DeFelice, L.J. 1997. *Drosophila* serotonin transporters have voltage-dependent uptake coupled to a serotonin-gated ion channel. *J. Neurosci.* **17:**3401–3411

Grewer, C., Watzke, N., Wiessner, M., Rauen, T. 2000. Glutamate translocation of the neuronal glutamate transporter EAAC1 occurs within milliseconds. *Proc. Natl. Acad. Sci. USA* **97:**9706–9711

Grossman, T.R., Nelson, N. 2003. Effect of sodium lithium and proton concentrations on the electrophysiological properties of the four mouse GABA transporters expressed in *Xenopus* oocytes. *Neurochem. Int.* **43:**431–443

Hazama, A., Loo, D.D.F., Wright, E.M. 1997. Presteady-state currents of the rabbit $Na^+/$glucose cotransporter (SGLT1). *J. Membrane Biol* **155:**175–186

Hilgemann, D.W., Lu, C.-C. 1999. GAT1 (GABA:Na^+:Cl^-) cotransport function. *Database reconstruction with an alternating access model. J. Gen. Physiol.* **114:**459–475

Itouji, A., Sakai, N., Tanaka, C., Saito, N. 1996. Neuronal and glial localization of two GABA transporters (GAT1 and GAT3) in the rat cerebellum. *Brain Res. Mol. Brain Res.* **37:**309–316

Kanner, B.I. 2003. Transmembrane domain I of the γ-aminobutyric acid transporter GAT-1 plays a crucial role in the transition between cation leak and transport modes. *J. Biol. Chem.* **278:**3705–3712

Keynan, S., Suh, Y.-J., Kanner, B.I., Rudnick, G. 1992. Expression of a cloned γ-aminobutyric acid transporter in mammalian cells. *Biochemistry* **31:**1974–1979

Kinney, G.A., Spain, W.J. 2002. Synaptically evoked GABA transporter currents in neocortical glia. *J. Neurophysiol.* **88:**2899–2908

Krogsgaard-Larsen, P., Frolund, B., Frylenvany, K. 2000. GABA uptake inhibitors. Design, molecular pharmacology and therapeutic aspects. Curr. Pharm. Des. **6:**1193–1209

Lester, H.A., Cao, Y., Mager, S. 1996. Listening to neurotransmitter transporters. *Neuron* **17:**807–810

Li, M., Farley, R.A., Lester, H.A. 2000. An intermediate state of the γ-aminobutyric acid transporter GAT1 revealed by simultaneous voltage clamp and fluorescence. *J. Gen. Physiol.* **115:**491–508

Lin, F., Lester, H.A., Mager, S. 1996. Single-channel currents produced by the serotonin transporter and analysis of a mutation affecting ion permeation. *Biophys. J.* **71:**3126–3135

Liu, Q.-R., López-Corcuera, B., Mandiyan, S., Nelson, H., Nelson, N. 1993. Molecular characterization of four pharmacologically distinct γ-aminobutyric acid transporters in mouse brain. *J. Biol. Chem.* **268:**2106–2112

Loo, D.D.F., Eskandari, S., Boorer, K.J., Sarkar, H.K., Wright, E.M. 2000. Role of Cl^- in electrogenic Na^+-coupled cotransporters GAT1 and SGLT1. *J. Biol. Chem.* **275:**37414–37422

Loo, D.D.F., Hazama, A., Supplisson, S., Turk, E., Wright, E.M. 1993. Relaxation kinetics of the $Na^+/$glucose cotransporter. *Proc. Natl. Acad. Sci. USA* **90:**5767–5771

Lu, C.-C., Hilgemann, D.W. 1999a. GAT (GABA:Na^+:Cl^-) cotransport function. Steady state studies in giant *Xenopus* oocyte membrane patches. *J. Gen. Physiol* **114:**429–444

Lu, C.-C., Hilgemann, D.W. 1999b. GAT1 (GABA:Na^+:Cl^-) cotransport function. Kinetic studies in giant *Xenopus* oocyte membrane patches. *J. Gen. Physiol.* **114:**445–457

MacAulay, N., Zeuthen, T., Gether, U. 2002. Conformational basis for the Li^+-induced leak current in the rat y-aminobutyric acid (GABA) transporter-1. *J. Physiol.* **544:**447–458

Mager, S., Kleinberger-Doron, N., Keshet, G.I., Davidson, N., Kanner, B.I., Lester, H.A. 1996. Ion binding and permeation at the GABA transporter GAT1. *J. Neurosci.* **16:**5405–5414

Mager, S., Min, C., Henry, D.J., Chavkin, C., Hoffman, B.J., Davidson, N., Lester, H.A. 1994. Conducting states of a mammalian serotonin transporter. *Neuron* **12:**845–859

Mager, S., Naeve, J., Quick, M., Labarca, C., Davidson, N., Lester, H.A. 1993. Steady states, charge movements, and rates for a cloned GABA transporter expressed in *Xenopus* oocytes. *Neuron* **10:**177–188

Matskevitch, I., Wagner, C.A., Stegen, C., Bröer, S., Noll, B., Risler, T., Kwon, H.M., Handler, J.S., Waldegger, S., Busch, A.E., Lang, F. 1999. Functional characterization of the betaine/γ-aminobutyric acid transporter BGT-1 expressed in *Xenopus* oocytes. *J. Biol. Chem.* **274:**16709–16716

Melamed, N., Kanner, B.I. 2004. Transmembrane domains I and II of the γ-aminobutyric acid transporter GAT-4 contain molecular determinants of substrate specificity. *Mol. Pharmacol.* **65:**1452–1461

Minelli., A., DeBiasi, S., Brecha, N.C., Zuccarello, L.V., Conti, F. 1996. GAT-3, a high-affinity GABA plasma membrane transporter, is localized to astrocytic processes, and it is not confined to the vicinity of GABAergic synapses in the cerebral cortex. *J. Neurosci.* **16:**6255–6264

Nelson, H., Mandiyan, S., Nelson, N. 1990. Cloning of the human brain GABA transporter. *FEBS Lett.* **269:**181–184

Nelson, N. 1998. The family of Na^+/Cl^- neurotransmitter transporters. *J. Neurochem.* **71:**1785–1803

Otis, T.S., Kavanaugh, M.P. 2000. Isolation of current components and partial reaction cycles in the glial glutamate transporter EAAT2. *J. Neurosci.* **20:**2749–2757

Panayotova-Heiermann, M., Loo, D.D.F., Lam, J.T., Wright, E.M. 1998. Neutralization of conservative charged transmembrane residues in the Na^+/glucose cotransporter SGLT1. *Biochemistry* **37:**10522–10528

Pastuszko, A., Wilson, D.F., Erecinska, M. 1982. Energetics of γ-aminobutyrate transport in rat brain synaptosomes. *J. Biol. Chem.* **257:**7514–7519

Quick, M.W. 2003. Regulating the conducting states of a mammalian serotonin transporter. *Neuron* **40:**537–549

Quick, M.W., Hu, J., Wang, D., Zhang, H.Y. 2004. Regulation of a γ-aminobutyric acid transporter by reciprocal tyrosine and serine phosphorylation. *J. Biol. Chem.* **279:**15961–15967

Radian, R., Kanner, B.I. 1983. Stoichiometry of sodium- and chloride-coupled γ-aminobutyric acid transport by synaptic plasma membrane vesicles isolated from rat brain. *Biochemistry* **22:**1236–1241

Richerson, G.B., Wu, Y. 2003. Dynamic equilibrium of neurotransmitter transporters: Not just for reuptake anymore. *J. Neurophysiol.* **90:**1363–1374

Roux, M.J., Supplisson, S. 2000. Neuronal and glial glycine transporters have different stoichiometries. *Neuron* **25:**373–383

Ruiz-Tachiquín, M.E., Sánchez-Lemus, E., Soria-Jasso, L.E., Arias-Montaño, J.A., Ortega, A. 2002. γ-aminobutyric acid transporter (BGT-1) expressed in human astrocytoma U373 MG cells: Pharmacological and molecular characterization and phorbol ester-induced inhibition. *J. Neurosci. Res.* **69:**125–132

Sacher, A., Nelson, N., Ogi, J.T., Wright, E.M., Loo, D.D.F., Eskandari, S. 2002. Presteady-state and steady-state kinetics, and turnover rate of the mouse γ-aminobutyric acid transporter (mGAT3). *J. Membrane Biol.* **190:**57–73

Sonders, M.S., Amara, S.G. 1996. Channels in transporters. *Curr. Opin. Neurobiol.* **6:**294–302

Sonders, M.S., Zhu, S.-J., Zahniser, N.R., Kavanaugh, M.P., Amara, S.G. 1997. Multiple ionic conductances of the human dopamine transporter: The actions of dopamine and psychostimulants. *J. Neurosci.* **17:**960–974

Wadiche, J.I., Arriza, J.L., Amara, S.G., Kavanaugh, M.P. 1995. Kinetics of a human glutamate transporter. *Neuron* **14:**1019–1027

Watzke, N., Bamberg, E., Grewer, C. 2001. Early intermediates in the transport cycle of the neuronal excitatory amino acid carrier EAAC1. *J. Gen. Physiol.* **117:**547–562

Whitlow, R.D., Sacher, A., Loo, D.D.F., Nelson, N., Eskandari, S. 2003. The anticonvulsant valproate increases the turnover rate of y-aminobutyric acid transporters. *J. Biol. Chem.* **278:**17716–17726

Wright, E.M., Loo, D.D.F., Turk, E., Hirayama, B.A. 1996. Sodium cotransporters. *Curr. Opin. Cell Biol.* **8:**468–473